

U.S. DEPARTMENT OF COMMERCE
National Technical Information Service

AD-A033 025

PHOTODISSOCIATION DYE LASER STUDIES AND HIGH
PRESSURE DISCHARGE CONDITIONING STUDIES

EXXON RESEARCH AND ENGINEERING COMPANY
LINDEN, NEW JERSEY

NOVEMBER 1976

AD A 033025

348070

EXXON RESEARCH AND ENGINEERING COMPANY

PHOTODISSOCIATION DYE LASER STUDIES AND
HIGH PRESSURE DISCHARGE CONDITIONING STUDIES

Final Technical Report

November 1976

Contract Period Covered: October 1, 1974 - September 30, 1976

ARPA Order Number	1806, Amendment 16
Program Code	6E 20
Contractor	Exxon Research & Engineering Company
Effective Date of Contract	October 1, 1974
Contract Expiration Date	September 30, 1976
Amount of Contract	\$199,997
Contract Number	N00014-73-C-0048
Principal Investigator	Abraham Kasdan (201-474-3947)
Co-Investigator	Robert J. L. Chimenti (201-474-2298)
Scientific Officer	Director, Physics Program ONR
Short Title of Work	Photodissociation Dye Laser and High Pressure Discharge Conditioning

The views and conclusions contained in this document are those of the authors and should not be interpreted as necessarily representing the official policies, either expressed or implied, of the Advanced Research Projects Agency or the U.S. Government.

Sponsored by:

Advanced Research Projects Agency
ARPA Order No. 1806

DDC
RECEIVED
DEC 9 1976

EXXON/GRUS.4BEOB.76

P. O. BOX 8 ■ LINDEN, NEW JERSEY 07036

REPRODUCED BY
NATIONAL TECHNICAL
INFORMATION SERVICE
U. S. DEPARTMENT OF COMMERCE
SPRINGFIELD, VA. 22161

EXHIBIT A
This document is to be released;
unclassified

EXXON

SECURITY CLASSIFICATION OF THIS PAGE (When Data Entered)

REPORT DOCUMENTATION PAGE		READ INSTRUCTIONS BEFORE COMPLETING FORM
1. REPORT NUMBER	2. GOVT ACCESSION NO.	3. RECIPIENT'S CATALOG NUMBER
4. TITLE (and Subtitle) Photodissociation Dye Laser Studies and High Pressure Discharge Conditioning Studies		5. TYPE OF REPORT & PERIOD COVERED Final Oct. 1, 1975-Sept. 30, 1976
7. AUTHOR(s) Abraham Kasdan and Robert J. L. Chimenti		6. PERFORMING ORG. REPORT NUMBER EXXON/GRUS.4BEOB.76
9. PERFORMING ORGANIZATION NAME AND ADDRESS Exxon Research and Engineering Company Government Research Laboratories--P.O. Box 8 Linden, New Jersey 07036		8. CONTRACT OR GRANT NUMBER(s) N00014-73-C-0048
11. CONTROLLING OFFICE NAME AND ADDRESS Physical Sciences Division Office of Naval Research--Dept. of the Navy 800 N. Quincy Street., Arlington, Virginia 22217		10. PROGRAM ELEMENT, PROJECT, TASK AREA & WORK UNIT NUMBERS ARPA Order No. 1806, Amend. 16--Program Code No. 6E 20
14. MONITORING AGENCY NAME & ADDRESS (if different from Controlling Office) Physical Sciences Division Office of Naval Research--Dept. of the Navy 800 N. Quincy St., Arlington, Virginia 22217		12. REPORT DATE November, 1976
		13. NUMBER OF PAGES 91
		15. SECURITY CLASS. (of this report) UNCLASSIFIED
		15a. DECLASSIFICATION/DOWNGRADING SCHEDULE None
16. DISTRIBUTION STATEMENT (of this Report) Approved for public release; distribution unlimited.		
17. DISTRIBUTION STATEMENT (of the abstract entered in Block 20, if different from Report) Approved for public release; distribution unlimited.		
18. SUPPLEMENTARY NOTES None		
19. KEY WORDS (Continue on reverse side if necessary and identify by block number) Photodissociation High Pressure Discharges Tunable Thermionic Emission Liquid Lasers		
20. ABSTRACT (Continue on reverse side if necessary and identify by block number) This report presents the results of two distinct experimental efforts. The photodissociation dye laser (PDL) studies represent an effort to develop a new class of tunable liquid lasers, in which laser action occurs between the electronic states of radical produced via photodissociation of specific classes of organic molecules in solution. Specifically, five molecules from a group known as the hexaarylethanes have been studied as potential laser media for the PDL scheme. Of these five molecules, only one - hexaphenylethane, exhibited radical fluorescence upon photodissociation.		

EXXON 1473

EDITION OF 1 NOV 65 IS OBSOLETE

UNCLASSIFIED

SECURITY CLASSIFICATION OF THIS PAGE (When Data Entered)

UNCLASSIFIED

SECURITY CLASSIFICATION OF THIS PAGE(When Data Entered)

Measurements of the maximum gain ($0.02/\text{cm}^{-1}$) and fluorescence yield (0.01) indicates that attainment of laser action in this system was not of practical interest.

The high pressure discharge conditioning studies involve an effort to generate and sustain spatially uniform discharges at pd values ≥ 1000 torr-cm by utilizing thermionic emission as the electron source. Using a heated cathode in a transverse discharge geometry, we have successfully demonstrated the attainment of long pulse, spatially uniform TEA discharges in several gases and gas mixtures with discharge currents lasting for 5 μsec .

UNCLASSIFIED

SECURITY CLASSIFICATION OF THIS PAGE(When Data Entered)

TABLE OF CONTENTS

	<u>Page</u>
I. INTRODUCTION AND SUMMARY	1
II. PHOTODISSOCIATION DYE LASER STUDIES	3
A. The Photodissociation Dye Laser Concept	3
1. Molecular Structure and Kinetics	3
2. General Chemical Properties of Free Radicals	6
3. Criteria for the Selection of Photodissociation Dye Laser Molecules	7
B. The Selected PDL Materials	8
1. Hexaphenylethane	10
a. Chemical Properties	10
b. Spectroscopic Properties	13
2. Properties of the Selected Hexaarylethane Derivatives	20
C. The Laser Excitation Sources	23
D. Rate Equation Analysis	26
E. Fluorescence Measurements	27
1. Hexaphenylethane	27
a. Excitation of the Visible Absorption Band	28
(1) Temperature Dependence of the Fluorescence Lifetime	28
(2) Temperature Dependence of the Fluorescence Intensity	33
b. Excitation of the UV Absorption Band	35
(1) Temperature Dependence of the Fluorescence Intensity	35
(2) Temporal Behavior of the Fluorescence	37
c. Absolute Intensity Measurements	38
d. Fluorescence Intensity as a Function of Excitation Wavelength	40
e. Photochemical Stability	43
2. Other PDL Molecules	45
F. Conclusions	50
III. HIGH PRESSURE DISCHARGE CONDITIONING STUDIES	52
A. Background	52
B. Breakdown Mechanisms on High Pressure Gases and Vapors	54
1. Townsend Breakdown	54
2. Streamer Breakdown	56
3. Considerations Affecting Spatial Uniformity	57

C.	Predischarge Conditioning by Thermionic Emission	61
D.	Experimental Effort and Results	62
E.	Discussion of Results	70
F.	Conclusions and Recommendations for Future Work	72
IV.	REFERENCES	74
	APPENDIX I - Preparation of PDL Candidates	76

LIST OF ILLUSTRATIONS

<u>Figure</u>	<u>Page</u>
1. Photodissociation Dye Laser Molecule Structure and Kinetics	5
2. Energy Level Structure of the Hexaphenylethane-Triphenylmethyl System	14
3. Mirror Image Symmetry of the Absorption and Fluorescence Spectra of the Triphenylmethyl Radical (Low Temperature Data)	16
4. Radical and Dimer Concentration as a Function of the Temperature	18
5. The Visible Absorption Spectrum of the Triphenylmethyl Radical at Room Temperature	19
6. The UV Absorption Spectrum of a Hexaphenylethane Solution at Room Temperature	21
7. UV Absorption Spectra of Selected Hexaarylethane Derivatives .	22
8. Cross-Sectional View of N ₂ Laser Assembly	25
9. Fluorescence Spectrum of a Hexaphenylethane Solution	29
10. Schematic Diagram of the Low Temperature Fluorescence Cell . .	31
11. Temperature Dependence of the Triphenylmethyl Radical Lifetime	32
12. Temperature Dependence of the Triphenylmethyl Fluorescence Intensity	34
13. Hexaphenylethane Fluorescence Intensity as a Function of Excitation Wavelength	41
14. The Effect of Photochemical Reactions on the Stability of the Triphenylmethyl Radical	44
15. Fluorescence Spectrum of Pentaphenylethane	46
16. Fluorescence Spectrum of 1- γ -Biphenyl-1,1,2,2 tetraphenylethane	47
17. Fluorescence Spectrum of 12-12' Bifluoradenyl	49

18. Spatial Development of Primary Electron Avalanche	58
19. The Heated Cathode Structure	65
20. Schematic Circuit for Thermionic Element Discharge Studies	66
21. The Effect of Thermionic Cathode on Discharge Uniformity	68

I. INTRODUCTION AND SUMMARY

This report presents results on two distinct topics of investigation. The first phase of our study, covering a period of 1½ years, represents a "proof of principle" effort to develop a new class of tunable liquid lasers operating in the visible region of the spectrum. The idea, termed the Photodissociation Dye Laser (PDL) concept, relies on laser action occurring between an excited electronic state and the ground electronic state of radicals produced by the photodissociation of specific classes of organic molecules in solution. This scheme is characterized by several potential advantages over conventional dye lasers. In particular, one expects no deleterious triplet level effects as well as long radiative lifetimes of the excited radical level.

For the purposes of this investigation, five promising candidates for the PDL active media were synthesized from a group of molecules known as the hexaarylethanes. Fluorescence measurements were performed on these molecules to assess their use as laser media.

The most promising molecule of the group appeared to be hexaphenylethane. Visible fluorescence from photodissociation of the dimer into excited state radicals was observed and long fluorescence lifetimes (~200 nsec) were measured. However, these lifetimes were observed only at low temperatures (-80°C). Room temperature lifetimes were measured to be short (~10 nsec). On the basis of absolute fluorescence intensity measurements, the potential optical gain coefficient for this system was estimated to be at most $\sim 0.02 \text{ cm}^{-1}$ under our N_2 laser pumping conditions. Experiments to achieve laser action in this system proved unsuccessful. Chemical reactivity problems associated with hexaphenylethanes were also

investigated. The remaining hexaarylethane molecules that were studied did not exhibit photodissociation into excited state radicals, and consequently were not of interest to the PDL scheme.

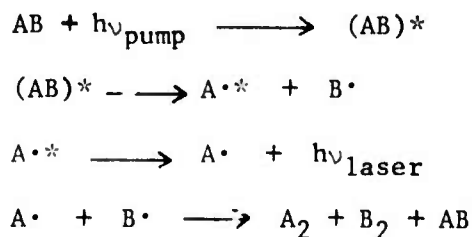
The second phase of our study, covering the remaining six months of the contract period, investigated the applicability of thermionic emission to sustain a long pulse, spatially uniform electrical discharge in high pressure (pd values ≥ 1000 torr-cm) laser media.

In these experiments, the cathode in a transverse discharge configuration was rapidly heated to high temperatures ($\sim 1500^\circ\text{C}$) just prior to the initiation of the discharge and the effects of the heated cathode on discharge uniformity in several high pressure gases were studied. Spatially uniform TEA discharges were successfully generated using this technique, and the results are consistent with calculations based on thermionic emission from the cathode. The primary advantage of this technique lies in its simplicity and low cost, when compared to existing e-beam and other preionization techniques.

II. PHOTODISSOCIATION DYE LASER STUDIES

A. The Photodissociation Dye Laser Concept

In its most general form, the photodissociation dye laser idea may be understood as follows: A stable molecule, AB, in solution is optically pumped to its first excited singlet state. The absorbed pump energy exceeds the molecule's dissociation energy and two radicals are formed upon dissociation. The excess energy is partitioned as electronic and vibrational excitation in one or both of the radicals A \cdot and B \cdot . In particular, we consider radical A \cdot to be electronically excited. A partial population inversion is produced between the first excited and the ground state of the radical. Laser action occurs in A \cdot and the resulting A \cdot and B \cdot ground state molecules are unstable against recombination. The processes may be written as:



In the final recombination step, not all of the radicals form the original molecule AB, but the dimeric forms A₂ and B₂ are also produced. Continuous laser action would then require replenishment of the starting material, AB. Let us consider in more detail the special case where A = B so that the starting molecule is dimeric.

1. Molecular Structure and Kinetics

The general energy level scheme for such a photodissociation dye laser molecule is shown schematically in Figure 1. The stable parent dimer, having no unpaired electrons, exhibits the usual singlet and triplet level

structure. The ground and excited electronic singlet levels are denoted by D_{S_0} , D_{S_1} , . . . and the triplet levels are denoted by D_{T_0} , D_{T_1} , . . .

The lowest electronic levels of the radicals, obtained from the symmetric photodissociation of the dimer, are shown adjacent to the dimer structure. The radical, having a single unpaired electron, exhibits a doublet structure. In the figure the radical ground state is shown displaced upward in energy from the dimer ground state by an amount equal to the dimer dissociation energy.

The vibrational level spacing in both the dimer and radical ranges between $150-1500\text{ cm}^{-1}$ while the rotational spacing ranges between $15-150\text{ cm}^{-1}$. Therefore, as in conventional dye lasers, a quasicontinuum exists for each electronic level comprised of the thermally broadened rotational and vibrational levels.

A characteristic of the photodissociation dye laser molecule is that the D_{S_1} and D_{T_0} levels in the dimer lie above the dimer dissociation energy. Consequently, upon optically pumping the dimer to D_{S_1} the molecule will undergo dissociation into two radicals. Dissociation may occur via two possible paths. The first is directly from the optically pumped D_{S_1} level. However, the D_{S_1} level may, in principle, undergo a rapid intersystem crossing to the D_{T_0} level. Dissociation of the dimer may then occur from this level.

Upon dissociation, the excitation energy is partitioned between a manifold of levels in the quasi-continuum of both the excited and ground state of the radical. The radical ground state initially has a negligible population; consequently, a partial inversion in the radical can be produced. The stimulated emission is tunable as in conventional dye lasers because

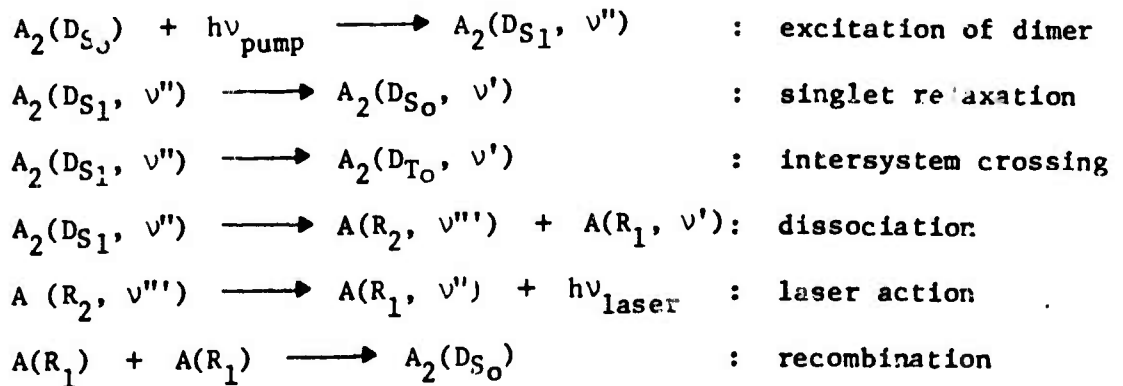
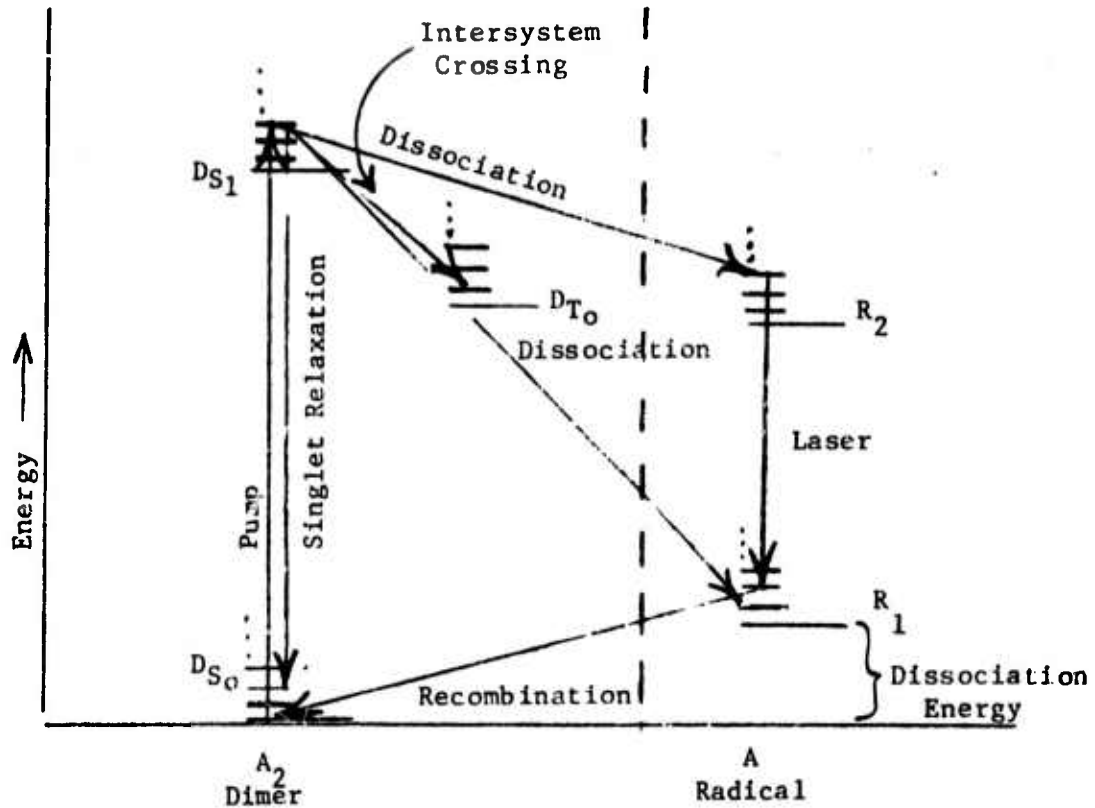


Figure 1. Photodissociation Dye Laser Molecule Structure and Kinetics

of the quasi-continuous distribution of the upper and ground levels. An interesting point is that for radicals considered suitable for the photodissociation dye laser, both the calculated and measured oscillator strengths for the first doublet-doublet electronic transition are often small. Thus, even though these transitions are allowed by the selection rules, they exhibit a partial "forbiddenness". Consequently, the radiative lifetime of the laser transitions can be expected to typically be a factor of a hundred times longer than in conventional dye lasers. This has been experimentally verified in some cases as will be discussed later. The longer lived upper laser level can permit a larger population density to be obtained and thereby allows the possibility of high power output.

The ability of the photodissociation dye laser to operate on a cw basis requires, as usual, that the depletion rate of the lower laser level exceed the radiative transition rate from the upper to the lower laser level. The lower laser level is the radical ground state which is unstable to recombination back to the original parent dimer. Thus, for a steady-state population inversion to be maintained, the radical combination rate must be greater than the laser transition radiative rate.

2. General Chemical Properties of Free Radicals

Recombination is only one of many possible reaction paths that can occur in a free radical system. Because they are characterized by an unbound electron, free radicals are usually very reactive. Consequently, competing processes can occur which make their production, handling, and any subsequent experimental analysis difficult. The primary radical reactions are:

(1) Disproportionation - two molecules of the radical are reduced at the expense of a third radical which is oxidized. This reaction can be catalyzed by heat or light.

(2) Irreversible Dimerization - this reaction results in an isomer of the original hexarylethane. It may be avoided by the rigorous exclusion of acids from the reaction system.

(3) Addition reactions - rapid absorption of atmospheric or dissolved oxygen to form colorless peroxide precipitates. Rigorous exclusion of oxygen is essential to minimize this reaction path.

The extent to which these reactions effect the chosen PDL materials will be elaborated in more detail later in this report.

3. Criteria for the Selection of Photodissociation Dye Laser Molecules

There are several requirements that an ideal photodissociation dye laser molecule should satisfy. Firstly, the dimer ground state must be thermally stable against dissociation at room temperature. Specifically, the ratio of the ground state radicals to ground state dimers at room temperature should typically be no greater than 10^{-4} . This will insure that there will be a negligible initial population in the lower laser level and that cryogenic operation will not be required.

A simple rate-equation model (see Section II-D) of the photodissociation dye laser based upon the dissociation of the dimer from the D_{S_1} level can be employed to determine the dominant rate processes. Such a model shows that the steady-state population (D_{S_1}) of excited singlet dimers is related to the population density of ground state dimers (D_{S_0}).

$$(D_{S_1}) = \frac{k_p}{k_1 + k_2 + k_D + 2k_D} (D_{S_0})$$

where

k_p = optical pumping rate

- k_1 = $D_{S_1} \longrightarrow D_{S_0}$ relaxation rate
 k_2 = $D_{S_1} \longrightarrow D_{T_0}$ intersystem crossing rate
 ${}^1k_D, {}^2k_D$ = dissociation rate into the R_1 and R_2 radical levels, respectively.

The R_2 upper laser level population density, (R_2) , obtained from the dissociation of the D_{S_1} level is given by:

$$(R_2) = \frac{{}^2k_D k_p}{\tau^{-1} (k_1 + k_2 + {}^1k_D + {}^2k_D)} (D_{S_0})$$

where τ^{-1} is the radiative lifetime of the upper laser level.

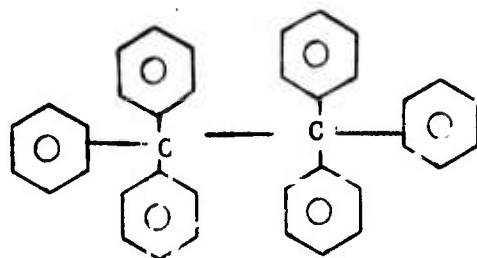
It can be seen from the above two equations that to obtain a large upper laser level population the pump rate must be large compared with the total depletion rate of the $D_{S_1} \longrightarrow D_{S_0}$ rates, the intersystem $D_{S_1} \longrightarrow D_{T_0}$ crossing rate, and the dissociation rate to R_1 and R_2 . In addition, the dissociation rate to R_2 should be large compared to the radiative decay rate through the laser transition. The fact that in some of the candidate molecules the proposed laser transition is partially forbidden helps to satisfy this requirement.

B. The Selected PDL Materials

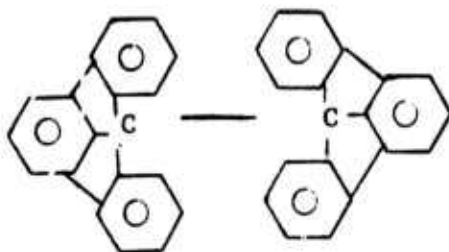
A class of organic compounds known as the hexaarylethanes exhibit some of the prerequisites necessary for a PDL active medium. For the purposes of this investigation five such compounds were selected, synthesized, and purified for further study. These five are*:

* The accepted structures of these dimer molecules are non-planar, and recent studies have shown them to possess a quinoid-type atomic arrangement. However, this does not affect in any way the proposed operation of the PDL scheme.

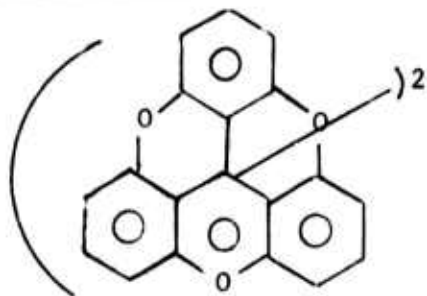
1. Hexaphenylethane



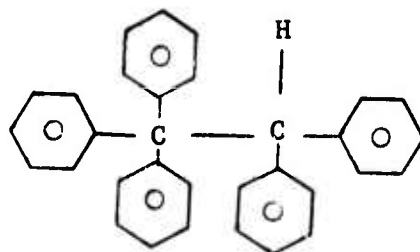
2. 12-12' Bifluoraderyl



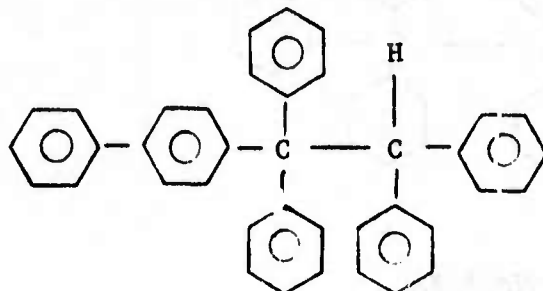
3. Sesquixanthryl



4. Pentaphenylethane



5. 1-p-Biphenyl-1,1,2,2-tetraphenylethane



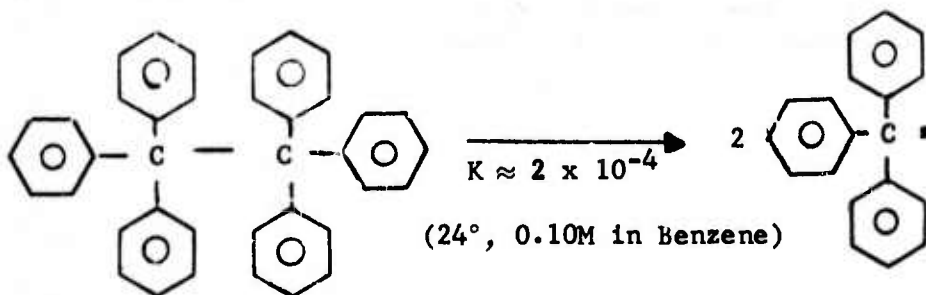
Details on the synthesis routes and experimental technique used in the preparation of these compounds are given in Appendix I. It should be pointed out that these materials are not conjugated double bond systems and therefore strictly speaking are not considered dyes according to the usual chemical usage of the word.

A summary of the relevant properties of each of the synthesized PDL molecules, based on a literature survey as well as our own initial observations, follows:

1. Hexaphenylethane

(a) Chemical Properties

Historically, hexaphenylethane is by far the most well characterized of the five synthesized compounds. It is solid at room temperature, and is readily dissolved in most organic solvents to form a yellow colored solution. This color is attributed to the formation, via thermal dissociation in solution, of the triphenylmethyl radical (1).



Hexaphenylethane
(Colorless Solid)

Triphenylmethyl Radical
(Yellow in Solution)

The existence of the radical has been proven by a multiplicity of analytical techniques. For example, cryoscopic molecular weight determinations of such compounds in solution have shown that the apparent molecular weights are well below that of the dimer. In addition, spectrophotometric measurements have established that solutions of the dimer do not obey Beer's law; the intensity of absorption increases with dilution as would be predicted for the dissociation of a colorless compound into a colored radical. Finally, absolute methods of radical detection - magnetic susceptibility and electron spin resonance spectroscopy - have shown beyond doubt the thermal dissociation of hexaphenylethane into ground state triphenylmethyl radicals.

Two factors determine the position of the hexaphenylethane-triphenylmethyl equilibrium: (a) Steric effects and (b) Radical stability.

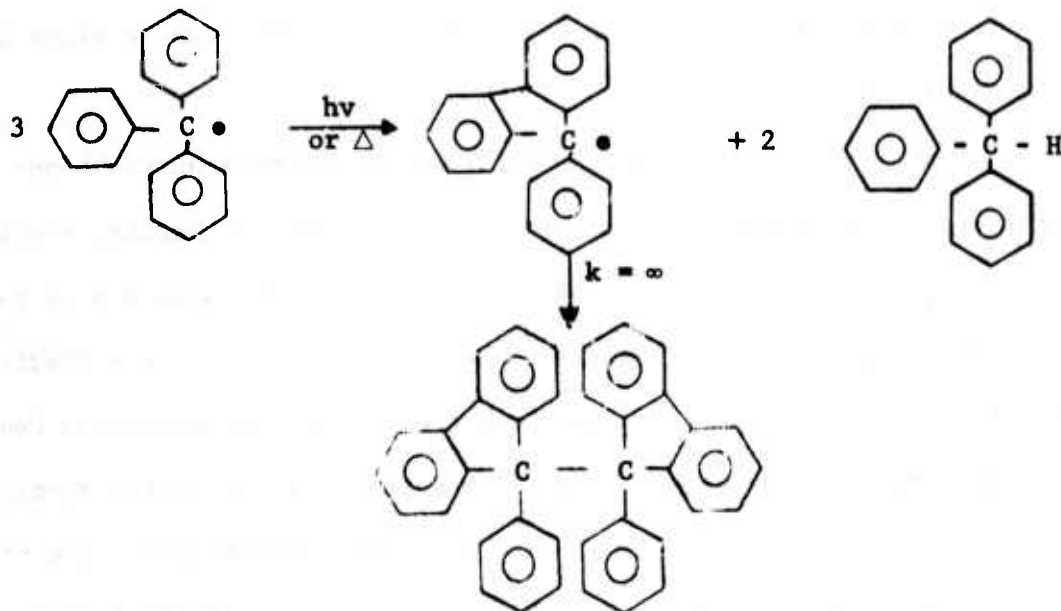
(a) Steric Effects - This factor favors the formation of radicals in two ways. First, there is a relief upon dissociation of the steric interactions in the ethane. In essence, the central carbon-carbon bond in the hexaphenylethane is weakened by the steric repulsion of the aromatic rings produced by interactions between the ortho-substituents. The bond weakening can be experimentally verified by comparison of the bond-length and strength of the central carbon-carbon bond in hexaphenylethane and the nonsterically-hindered ethane:

	<u>Hexaphenylethane</u>	<u>Ethane</u>
Bond Length	1.58 Å	1.54 Å
Bond Strength	11.5 kcal/mole	85 kcal/mole

The second steric effect is typified by a steric hindrance to recombination once a radical is formed.

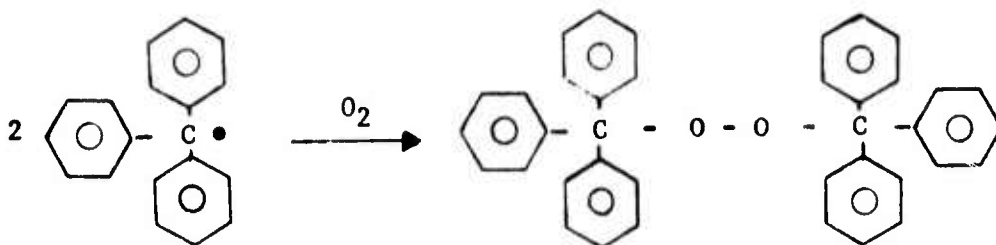
(b) Radical Stability - The stability of the triphenylmethyl radical is provided by a resonance stabilization effect resulting from the delocalization of the free electron throughout the three aromatic rings of the structure.

As mentioned earlier, a number of chemical properties act to complicate the use of hexaphenylethane as a PDL active media candidate. These properties arise from the reactivity of the produced radicals. The first of these is its propensity towards disproportionation. This transformation is promoted by heat or light and is illustrated below:



In essence, two molecules of the radical become reduced at the expense of a third radical which is oxidized. For the triphenylmethyl radical, the products are triphenylmethane and the dehydro-dimer of 9-phenylfluorene. Measurements of the effect of this photochemical or thermal degradation on the use of hexaphenylethane as a laser media will be present later in this report.

The second deleterious reaction path which occurs when radicals are produced is the addition reaction. This involves the rapid absorption of atmospheric oxygen to form colorless triphenylmethyl peroxides:



As the radicals react, more dissociation must occur in order to maintain the dimer-radical equilibrium constant. In this way, a continuous depletion of both the radical and dimer concentration occurs until all the hexaphenylethane in solution has reacted to form the peroxide precipitate. However, careful preparation under vacuum conditions and subsequent storage and handling under a nitrogen atmosphere has yielded solutions that are quite stable with respect to such reactions. Spectrophotometric measurements of the radical concentration over a period of time in solutions we have prepared indicate a decrease of only several percent per week; and this decrease is probably due primarily to thermal disproportionation.

(b) Spectroscopic Properties

The reported major bands in the electronic absorption spectra of hexaphenylethane and the triphenylmethyl radical are shown below along with the measured extinction coefficients (2):

<u>Hexaphenylethane</u>	<u>Triphenylmethyl Radical</u>
$\lambda_{\max} = 3150 \text{ \AA}$ (using KBr pellet technique)	$\lambda_{\max} = 3450 \text{ \AA}$, $\epsilon = 11,000$
$\lambda_{\max} = 3130 \text{ \AA}$ (dissolved in cyclohexane)	$\lambda_{\max} = 5100 \text{ \AA}$, $\epsilon = 210$
	(both in cyclohexane)

The major absorption bands can be associated with electronic transitions. The resulting dimer and radical energy level structure is shown in Figure 2. The first excited singlet level of the dimer, D_{S1} , is $\sim 31,750 \text{ cm}^{-1}$ above the ground state. The activation energy for dissociation

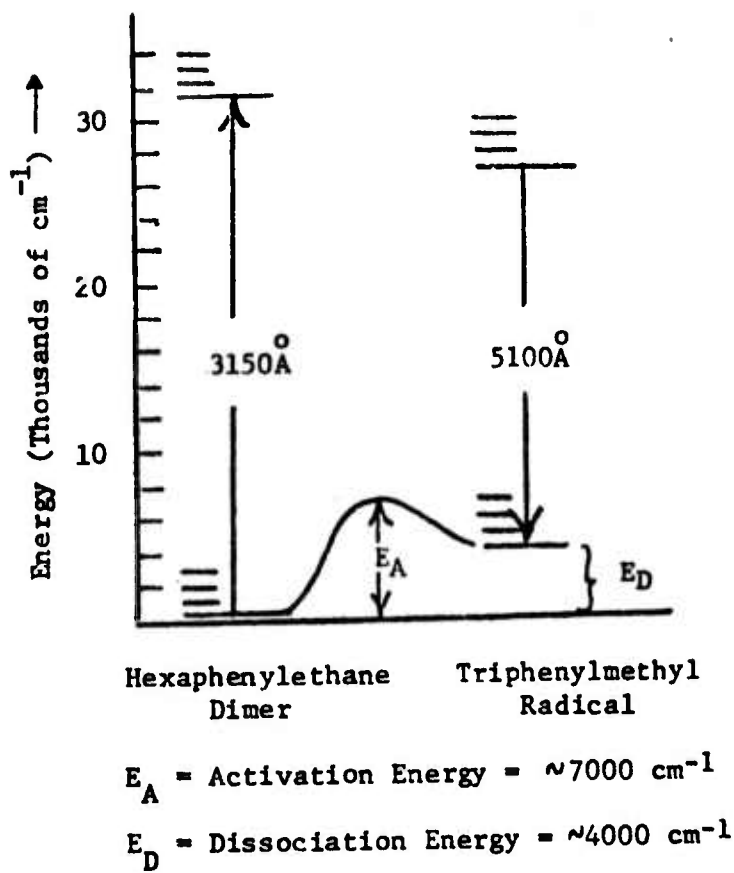


Figure 2. Energy Level Structure of the Hexaphenylethane-Triphenylmethyl System.

is $\sim 7000 \text{ cm}^{-1}$ (3) while the dissociation energy is $\sim 4000 \text{ cm}^{-1}$ (4). The ground vibrational level of the first excited electronic state in the triphenylmethyl radical lies at $19,410 \text{ cm}^{-1}$ and the second excited electronic level is at $\sim 29,000 \text{ cm}^{-1}$ above the ground state.

The mirror image symmetry of the absorption and fluorescence bands is illustrated in Figure 3. The spectra were originally reported by Lewis et al. (5) and were measured by suddenly cooling a solution of hexaphenylethane in EPA (5 parts ether, 5 parts isopentane, and 2 parts ethanol by volume) to liquid N_2 temperature (-190°C). It was reported that rapid cooling preserved the highly colored radicals in the clear EPA glass, and that under these conditions, there was no evidence of disproportionation. Unfortunately, no details regarding the measurement techniques used in taking the fluorescence data were presented--nor was the excitation source or wavelength described.

More recently, Okamura et al. (6) performed time resolved fluorescence measurements on the triphenylmethyl and other methyl-substituted radicals which were trapped in rigid solvents at low temperature. The triphenylmethyl radical was prepared by the photolysis of triphenylmethane molecules at -190°C in a quartz cell using a low pressure mercury lamp. An N_2 laser emitting a 10 nsec, 40 kw peak power pulse at 3371 \AA was used as the excitation source. The fluorescence decay consisted of a single exponential with the measured decay times being 280 nsec with ethyl alcohol as solvent, and 330 nsec using isopentane as the solvent. The very long fluorescence lifetimes were taken as evidence that the first doublet-doublet electronic transition in the radical has a forbidden character, although such transitions are allowed by the usual selection rule considerations. The possibility that the observed lifetimes were actually longer than the natural lifetimes because of complex formation of the excited state with the solvent, was ruled out by the fact that the difference of measured lifetimes in polar and nonpolar solvents was not appreciable.

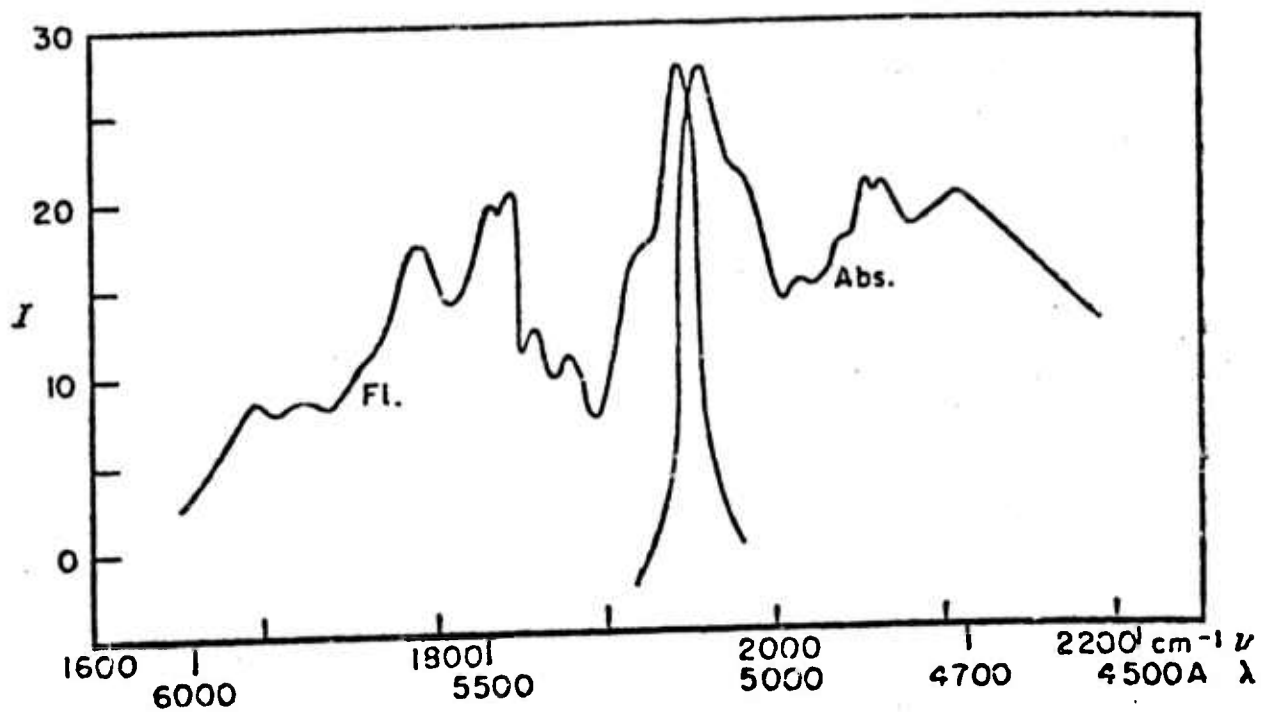


Figure 3. Mirror Symmetry of Absorption and Fluorescence Bands of the Triphenylmethyl Radical (in EPA mixed solvent at -190°C). Ref. (5).

In the present investigation, solutions of hexaphenylethane dissolved in iso-octane (a UV-transmitting solvent) have been studied. As already pointed out, hexaphenylethane in solution undergoes appreciable thermal decomposition at room temperature into triphenylmethyl radicals. For example, what would be a 10^{-3} M solution of hexaphenylethane in the absence of thermal decomposition actually results in $\sim 25\%$ dissociation at room temperature--yielding $\sim 7.5 \times 10^{-4}$ M hexaphenylethane and $\sim 5 \times 10^{-4}$ M triphenylmethyl radical.

Since the dissociation energy, H , is known (11.8 kcal/mole) the equilibrium constant K can be calculated as a function of temperature ($K = Ae^{-H/RT}$) if its value at one temperature is known. Since $K \equiv \frac{[R]^2}{[D]}$, where $[R]$ and $[D]$ are the radical and dimer concentrations respectively, the resulting concentrations can be calculated as a function of temperature for a given initial dimer concentration $[D_0]$. The results of such a calculation are shown in Figure 4. The measured value of $K = 4.1 \times 10^{-4}$ at 20°C was used (4). Although this value was obtained using benzene as solvent, it has been shown (4) that solvent variations do not change the value of the equilibrium constant significantly.

The solutions we have prepared, using the method outlined in Appendix I, have resulted in $\sim 2 \times 10^{-3}$ M radical concentration at room temperature. This value is obtained from an absorbance measurement in the visible (see Figure 5), using the previously measured value of the extinction coefficient $\epsilon = 210 \text{ l-mole}^{-1}\text{-cm}^{-1}$ (2) for the peak of the visible triphenylmethyl absorption ($\sim 5150 \text{ \AA}$). Note that except for the absence of much of the structure evident in the low temperature visible absorption data (Figure 3), the room temperature absorption data is otherwise identical.

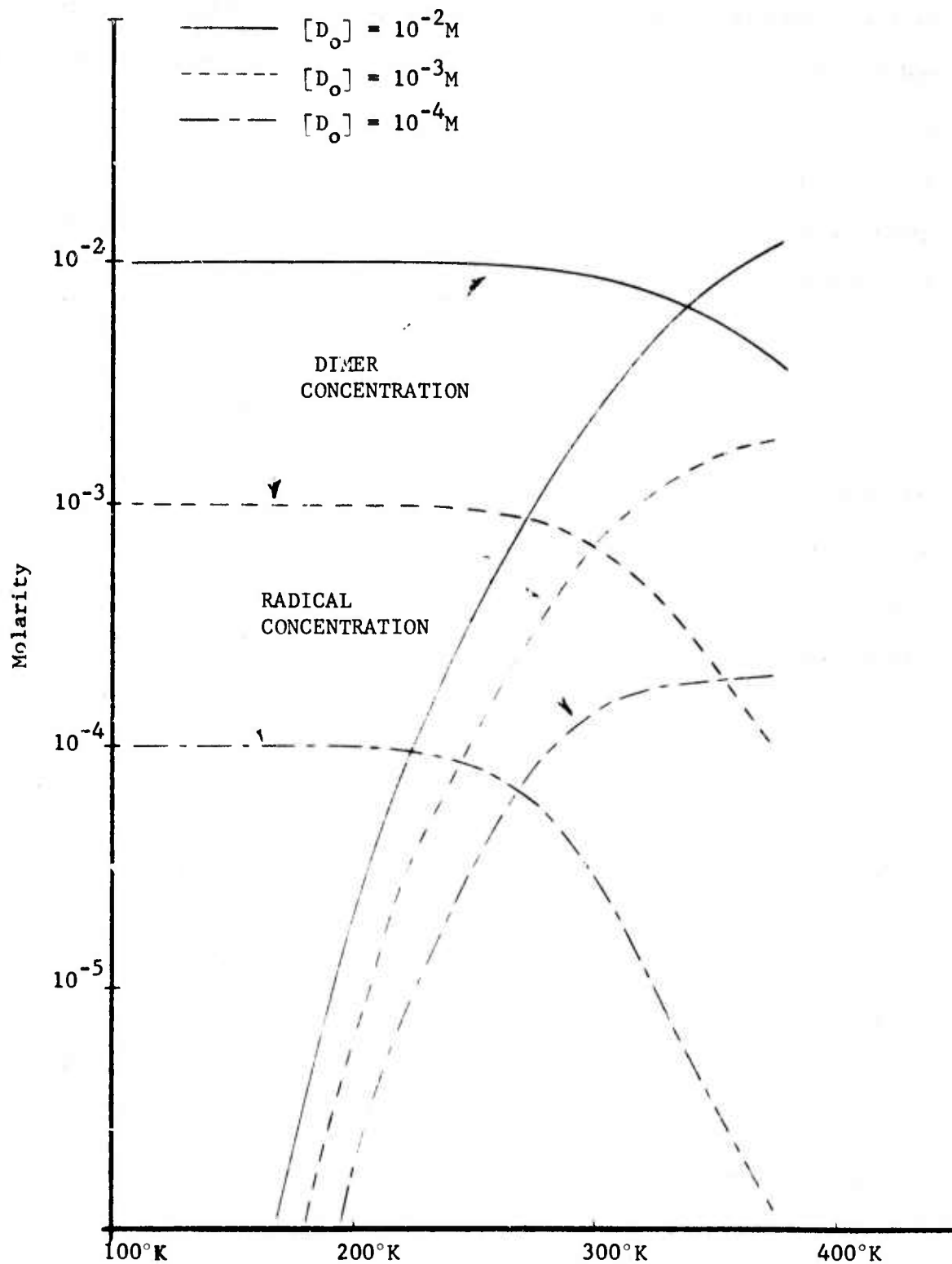


Figure 4: Triphenylmethyl Radical and Hexaphenylethane Dimer Concentrations in Solution as a Function of Temperature and Undissociated Dimer Concentration.

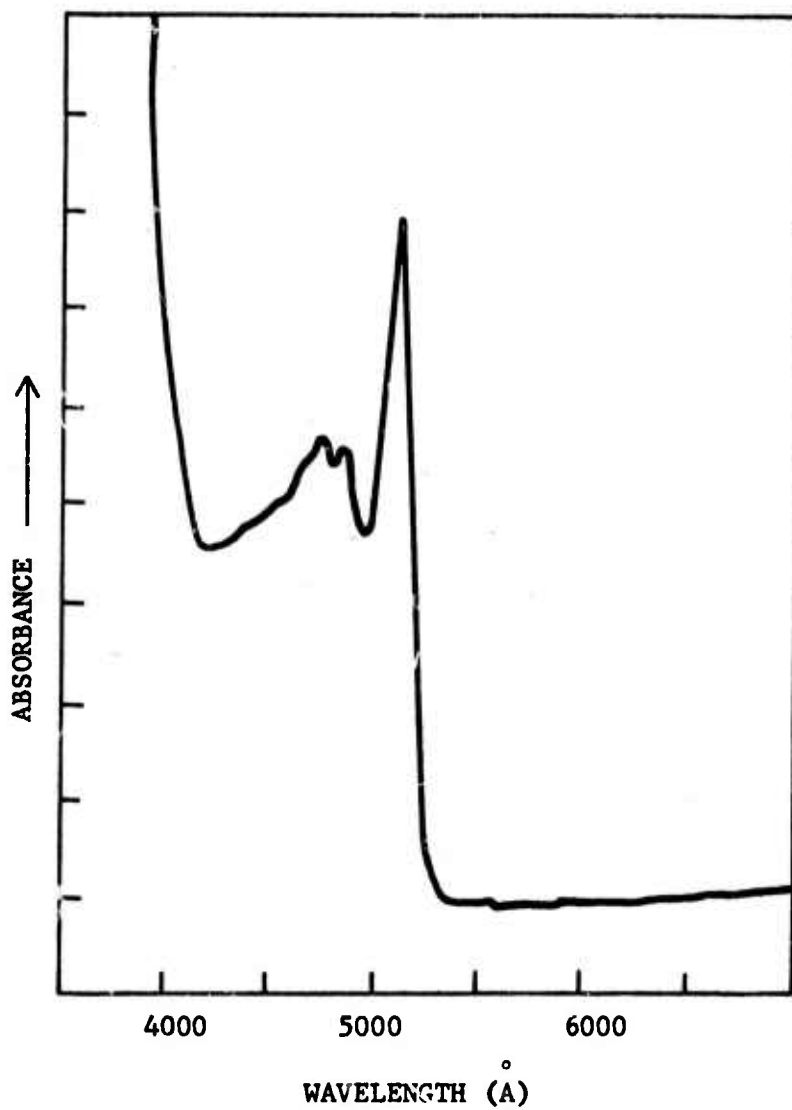


Figure 5. Visible Absorption Spectrum of the Triphenylmethyl Radical Taken at Room Temperature. (Hexaphenylethane in Iso-octane).

For wavelengths $< 3500 \text{ \AA}$, the absorption of the hexaphenylethane solutions at the concentrations used in our experiment is $> 99\%$. If dilute solutions are prepared, the UV absorption curve shown in Figure 6 is obtained. The absorption is characterized by a broad feature with a peak at $\sim 3350 \text{ \AA}$. No structure is resolvable although a shoulder on the short wavelength side is evident. It is believed that this feature is due to the unresolved combination of dimer absorption (reported in the literature to peak at $\sim 3150 \text{ \AA}$) and radical absorption to a second excited state (reported to peak at $\sim 3450 \text{ \AA}$).

2. Properties of the Selected Hexaarylethane Derivatives

12-12' Bifluoradenyl

This material is completely stable at room temperature, i.e., essentially no radicals are thermally produced. The UV absorption spectrum we have measured is shown in Figure 7A. The dimer absorption feature is the broad plateau region centered at $\sim 2800 \text{ \AA}$. We have calculated the extinction coefficient ϵ to be $40,000 \text{ l-mole}^{-1}\text{-cm}^{-1}$ at 2800 \AA .

Evidence has been sought in the literature for the possible dissociation of 12-12' bifluoradenyl into fluoradenyl radicals. However, published attempts, including ESR measurements, have yielded negative results.

We have looked for a color change indicative of the existence of thermally produced radicals upon heating a solution to 150°C . Again the results were negative. However, this does not exclude the possibility of radical production during photodissociation.

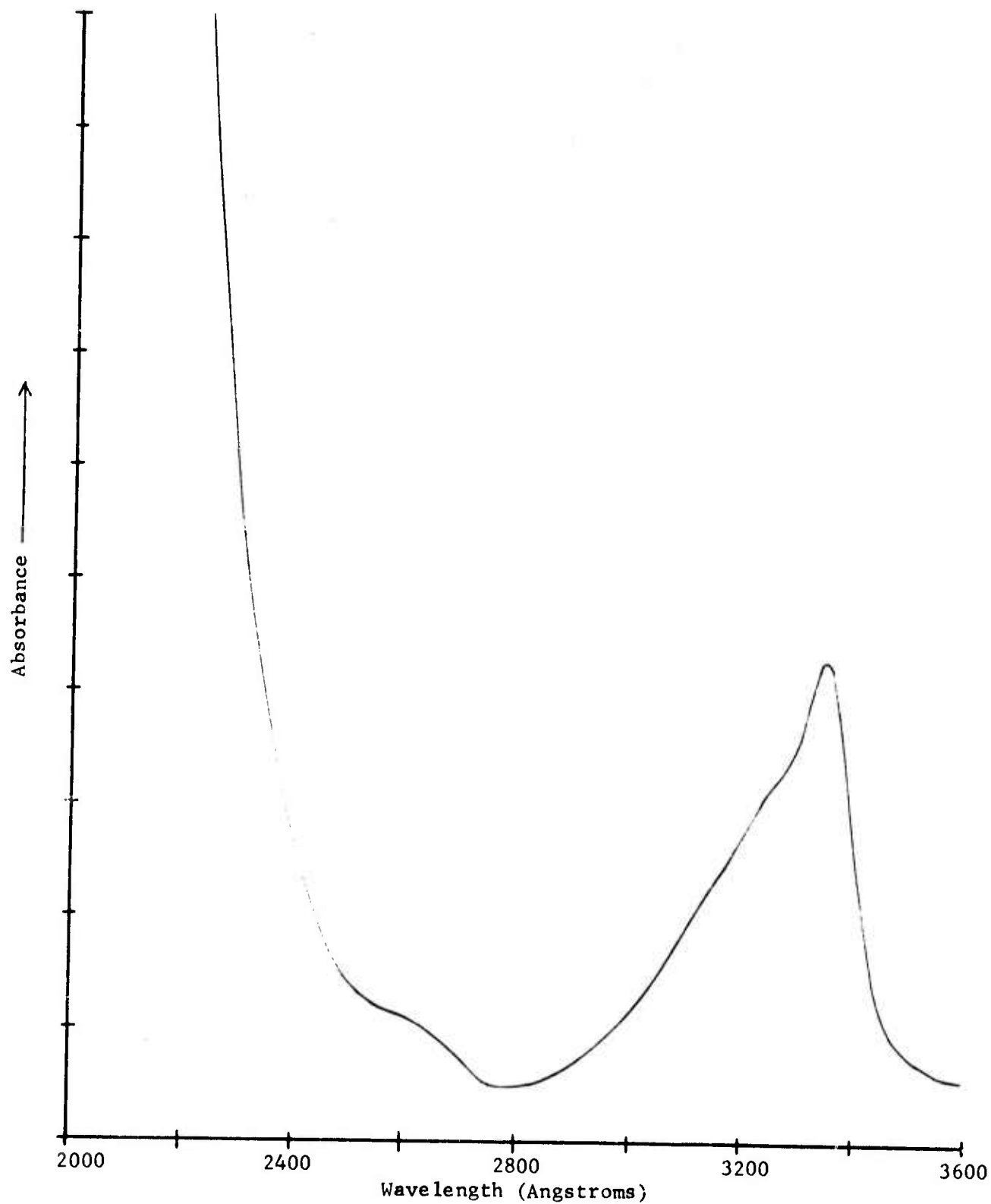
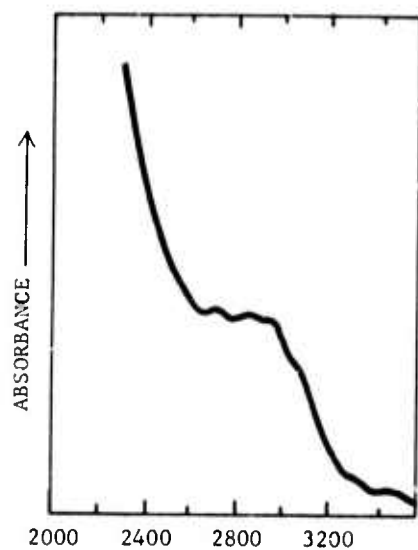
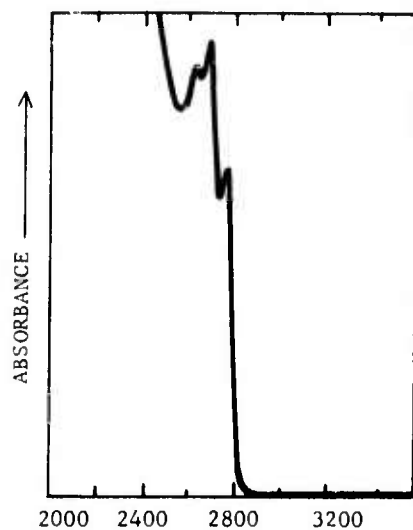


Figure 6. UV Absorption Spectrum of Hexaphenylethane Solution at Room Temperature (in iso-octane).



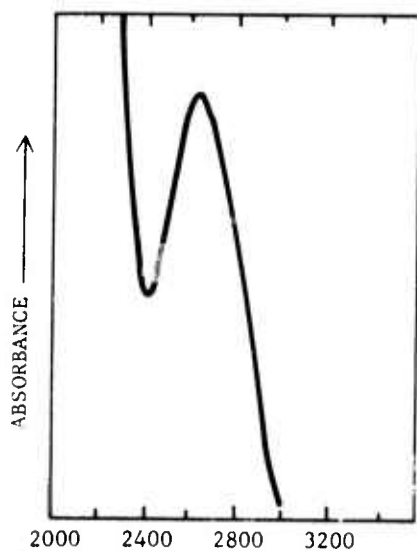
(A) 12-12' BIFLUORADENYL

$$\epsilon = 40,000 \text{ -mole}^{-1}\text{-cm}^{-1}$$



(B) PENTAPHENYLETHANE

$$\epsilon = 1800 \text{ -mole}^{-1}\text{-cm}^{-1}$$



(C) 1-p-BIPHENYL-1,1,2,2-TETRAPHENYLETHANE

$$\epsilon = 25,000 \text{ , mole}^{-1}\text{-cm}^{-1}$$

WAVELENGTH (A)

Figure 7. UV Absorption Spectra of PDL Molecules - the extinction coefficients at the peak of the dimer absorption bands are given.

Sesquixanthryl

This material is completely stable as dimer at room temperature. At elevated temperature ($\sim 100^\circ\text{C}$) thermal production of radicals has been observed both by noting a color change when a solution is heated as well as by ESR techniques. However, solubility studies we have performed indicate that sesquixanthryl is very insoluble in every common organic solvent except methyl benzoate. Methyl benzoate, however, absorbs strongly at $\leq 3300 \text{ \AA}$ and therefore no UV data on the dimer could be obtained.

Pentaphenylethane

We have obtained the UV absorption spectrum of pentaphenylethane as shown in Figure 7B. It exhibits a peak absorption at 2670 \AA with an extinction coefficient $\epsilon = 1800 \text{ l-mole}^{-1}\text{-cm}^{-1}$. Historically, color attributed to radical formation has been observed in an ethyl benzoate solution at $\sim 100^\circ\text{C}$ (7).

1-p-Biphenyl-1,1,2,2-tetraphenylethane

The measured UV absorption spectrum is shown in Figure 7C. Peak absorption occurs at 2600 \AA with an extinction coefficient $\epsilon = 25,000 \text{ l-mole}^{-1}\text{-cm}^{-1}$. Color change indicative of radical formation has been observed in heated solution ($\sim 100^\circ\text{C}$) (7).

C. The Laser Excitation Source

The dimer absorption bands of all the PDL molecules synthesized under this program are in the UV region covering a range of $2600\text{-}3200 \text{ \AA}$. In order to study the photodissociation of such systems a tunable UV laser source was assembled.

The 3371 \AA output of a N_2 laser was used to pump a Moletron DL 300 Dye Laser. Frequency doubling the dye output by means of KDP crystals provides a UV probe with a tunable output range of $2600\text{-}3700 \text{ \AA}$.

Measured operating characteristics of the system are:

	<u>Energy/Pulse</u>	<u>Time Duration</u>	
N ₂ Laser	~ 5 mj	8-10 ns	System Rep. Rate: 1-10 pps
Dye Laser	0.5-0.7 mj	5 ns	
Doubled Output	10-40 μ j	5 ns	

The nitrogen laser

ward, Ehlers, & Lineberger (8). Basically, energy is stored in two 0.1 μ f Tobe Deutchman disc capacitors connected in series. This energy is then transferred by an EGG HY 3202 thyatron switch to a low inductance transmission line consisting of 100 Belden YK-217 17.2 cables connected in parallel across the discharge electrode. A cross-sectional view of the laser assembly is shown in Figure 8.

The length of the active discharge region is 150 cm. To insure a uniform discharge along this length an N₂ flow transverse to both the discharge direction and optic axis has been incorporated in the design. Nitrogen gas enters through evenly spaced holes positioned along the length of the ground electrode, and is pumped out through similarly positioned holes as shown in Figure 8.

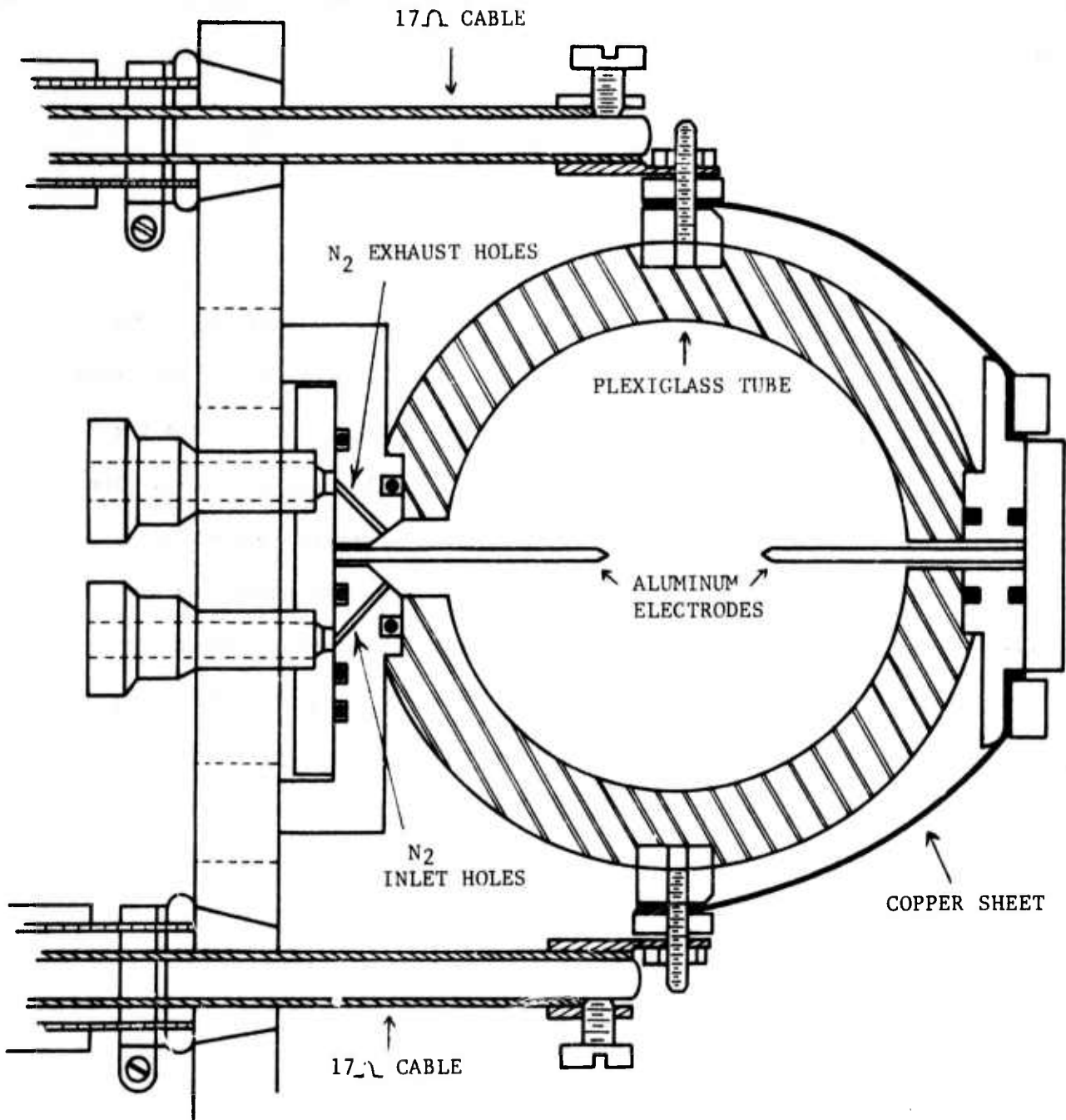
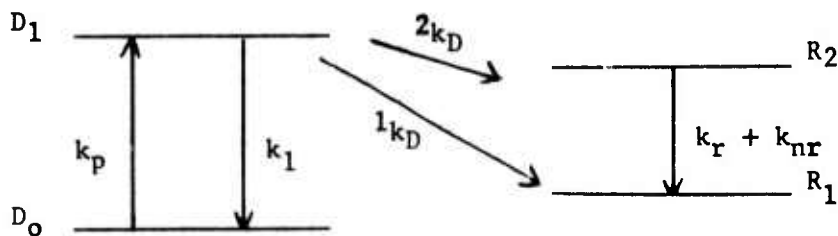


Figure 8. Cross-sectional view of N₂ laser assembly.

D. Rate Equation Analysis

In order to evaluate what information time-resolved measurements of absorption and fluorescence can yield about the rates involved in the PDL scheme, the appropriate rate equations have been solved. Such an analysis has been performed assuming the following model:



The first excited dimer is pumped with a rate constant k_p . The total decay rate out of D_1 by all processes except dissociation is described by k_1 , and the dissociation rates into the upper radical state R_2 and the ground radical state R_1 are characterized by $2k_D$ and $1k_D$ respectively. The processes contributing to k_1 include fluorescence, internal conversion and intersystem crossing. In the model for which the rate equations are written the molecules in D_1 which undergo intersystem crossing return to D_0 . The radical decay is characterized by the sum of a radiative term k_r and a non-radiative term, k_{nr} . Radical recombination is neglected here so that the resulting rate equations remain linear.

Four equations may be written:

$$\frac{dD_0}{dt} = -k_p D_0 + k_1 D_1$$

$$\frac{dD_1}{dt} = k_p D_0 - (k_1 + k_D) D_1 \text{ where } k_D = 1k_D + 2k_D$$

$$\frac{dR_2}{dt} = 2k_D D_1 - (k_r + k_{nr}) R_2$$

$$\frac{dR_1}{dt} = 1k_D D_1 + (k_r + k_{nr}) R_2$$

where, D_0 , D_1 , R_2 , and R_1 , denote the time varying population densities of the respective states.

The equations have been solved assuming $k_p = \text{constant}$ for $0 \leq t \leq t_p$ and $k_p = 0$ for $t > t_p$, with the boundary conditions $D_0(0) = \text{constant}$, $D_1(0) = 0$, $R_2(0) = 0$, and $R_1(0) = 0$. This yields the time behavior after pumping with a rectangular pulse, of a system which initially consists of all ground state dimers. Several important conclusions can be drawn from the results. After the pump pulse has terminated, solution of the equations shows that the time rate of change of the upper radical level has the form:

$$R_2(t) = A e^{-(k_r + k_{nr})(t-t_p)} + B e^{-(k_1 + k_D)(t-t_p)} \quad t > t_p$$

Since the intensity of fluorescence decay is proportional to the population density of the decaying state, the fluorescence decay rate of the upper radical state after the dimer absorption band has been pumped should exhibit the above time dependence. If the PDL system behaves according to our model, analysis of this decay will yield the values $(k_r + k_{nr})$ and $(k_1 + k_D)$.

Fluorescence decay of the upper radical state may also be monitored after pumping the radical absorption band. In this case, since there is no dimer contribution, the observed decay rate will yield the value $(k_r + k_{nr})$. Note that both of the above experiments must be performed in order to obtain and identify the $(k_1 + k_D)$ rate and the $(k_r + k_{nr})$ rate.

E. Fluorescence Measurements

1. Hexaphenylethane

Since hexaphenylethane is the most well characterized of the five synthesized PDL molecules from both a chemical and spectroscopic viewpoint, this molecule was the first to be studied by us as a potential active media for a PDL laser.

It was initially observed by us, that when a room temperature solution of hexaphenylethane is irradiated with the N₂ laser (3371 Å), a bright greenish-yellow fluorescence results. The fluorescence spectrum was obtained with a Spex 1 meter spectrometer by signal averaging the photomultiplier pulses with a boxcar integrator, and is shown in Figure 9. The spectrum corresponds to the reported low temperature spectrum of the triphenylmethyl radical, although the multiple peaks exhibited in the low temperature spectrum are not evident. The broad feature at ~4000 Å is not due to either hexaphenylethane or the triphenylmethyl radical. Its significance will be discussed later in Section IIE-1e.

a. Excitation of the Visible Absorption Band

(1) Temperature Dependence of the Fluorescence Lifetime

As previously mentioned, the reported fluorescence lifetime of the triphenylmethyl radical at 77°K is ~ 300 ns (6). However, the initial lifetime measurements we performed at room temperature yielded ~ 10 ns lifetimes at all points on the observed spectrum (5150 Å-6000 Å). These measurements were made by exciting the first absorption band of the thermally generated radicals directly by a 5 ns dye laser pulse at 5150 Å. Excitation at this wavelength, rather than in the UV, precludes any complicating effects arising from simultaneous dimer excitation since the visible absorption band is due exclusively to the presence of the triphenylmethyl radical. The above equation for R₂(t) then reduces to:

$$R_2(t) = A_e - (k_r + k_{nr})(t-t_p) \quad t > t_p$$

The reason for the difference in the two lifetime measurements is due to the temperature dependent non-radiative decay rate, k_{nr}. At low temperatures, the non-radiative rate is reduced, thereby increasing the observed lifetime. In order to achieve maximum possible inversion as a laser media, a PDL system should operate in a temperature regime where the fluorescence

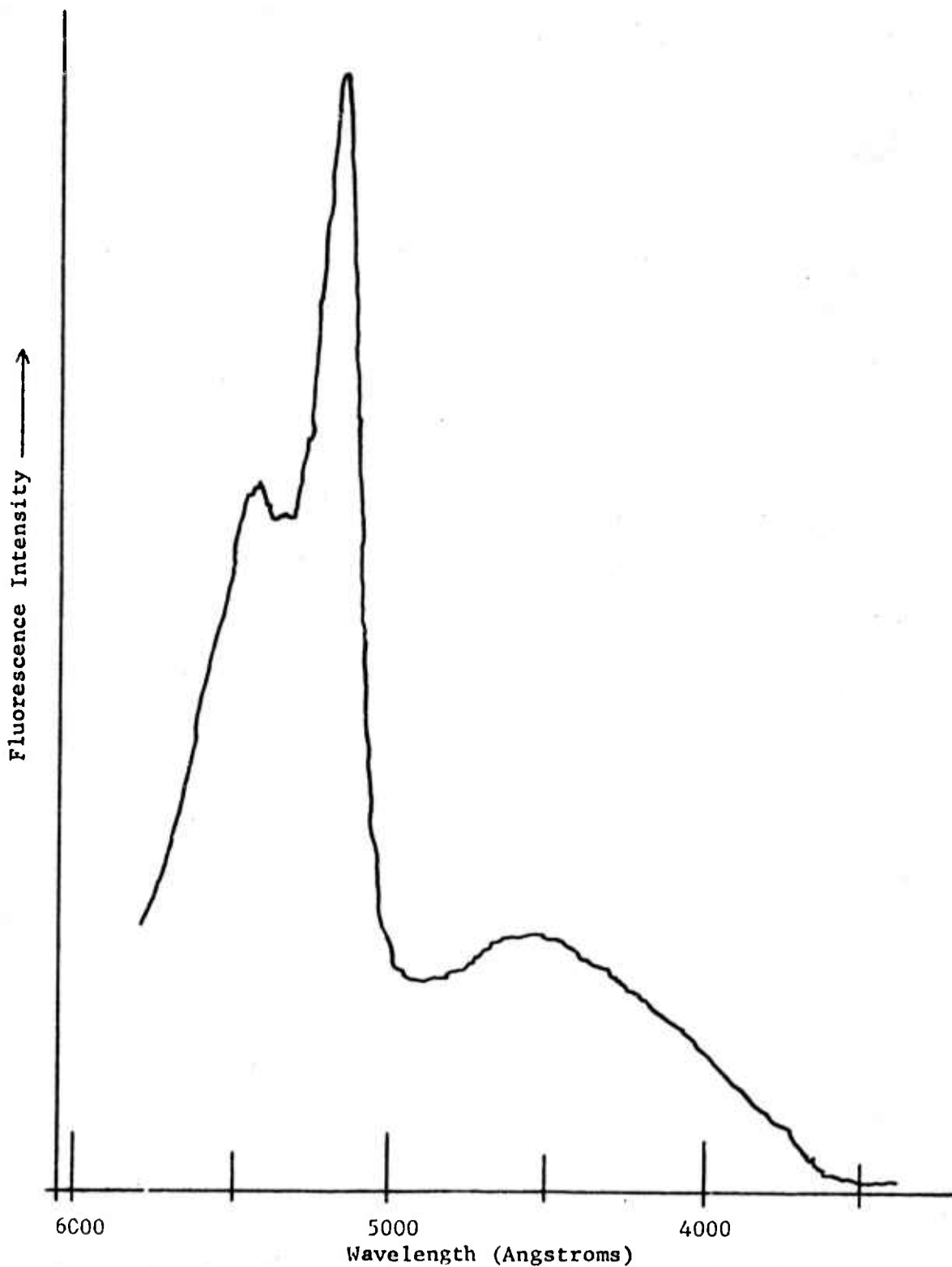


Figure 9. Room Temperature Fluorescence of a Hexaphenylethane Solution (in iso-octane). The Characteristic Triphenylmethyl Radical Fluorescence is seen as well as a Broad Feature in the Blue. Excitation is with an N_2 Laser (3371 Å).

lifetime is as long as possible. A temperature dependence study of the fluorescence lifetime was therefore undertaken.

In order to perform such measurements, a simple fluorescence cell capable of being cooled and operated at low temperature without moisture condensation problems on the windows was devised. A schematic diagram of the cell is shown in Figure 10. A conventional jacketed quartz spectrophotometer cell was set up so that cooled N₂ gas flowed through the jacket surrounding the hexaphenylethane. A thermocouple placed in the solution provided for temperature measurement. The cell was filled with the hexaphenylethane in a dry box under an N₂ atmosphere and subsequently sealed to prevent oxygen from reacting with the radicals. The entire cell was surrounded by a plexiglass cylinder with appropriately positioned quartz windows so that the fluorescence could be viewed at right angles to the excitation light. Room temperature dry nitrogen gas was continuously flowed through this outer chamber so that water vapor which would otherwise condense on the cell windows was eliminated from the cell. By controlling the flow of the cold N₂ gas, temperature stability could easily be maintained to $\pm 1^\circ\text{C}$. Using this configuration fluorescence data from room temperature down to -90°C were obtained. The solution was excited at the peak of the radical absorption band in the visible (5150 Å) by a 5 ns dye laser pulse. The fluorescence was passed through a Perkin-Elmer monochromator and was monitored at right angles by an RCA C31025C photomultiplier tube and a 7904 Tektronix oscilloscope.

All the fluorescence decay curves were analyzed to be single exponentials, as expected. The fluorescence lifetime was seen to increase rapidly from the room temperature value of ~ 10 ns to greater than 200 ns at -90°C . A compilation of the data from a number of different runs is shown in Figure 11.

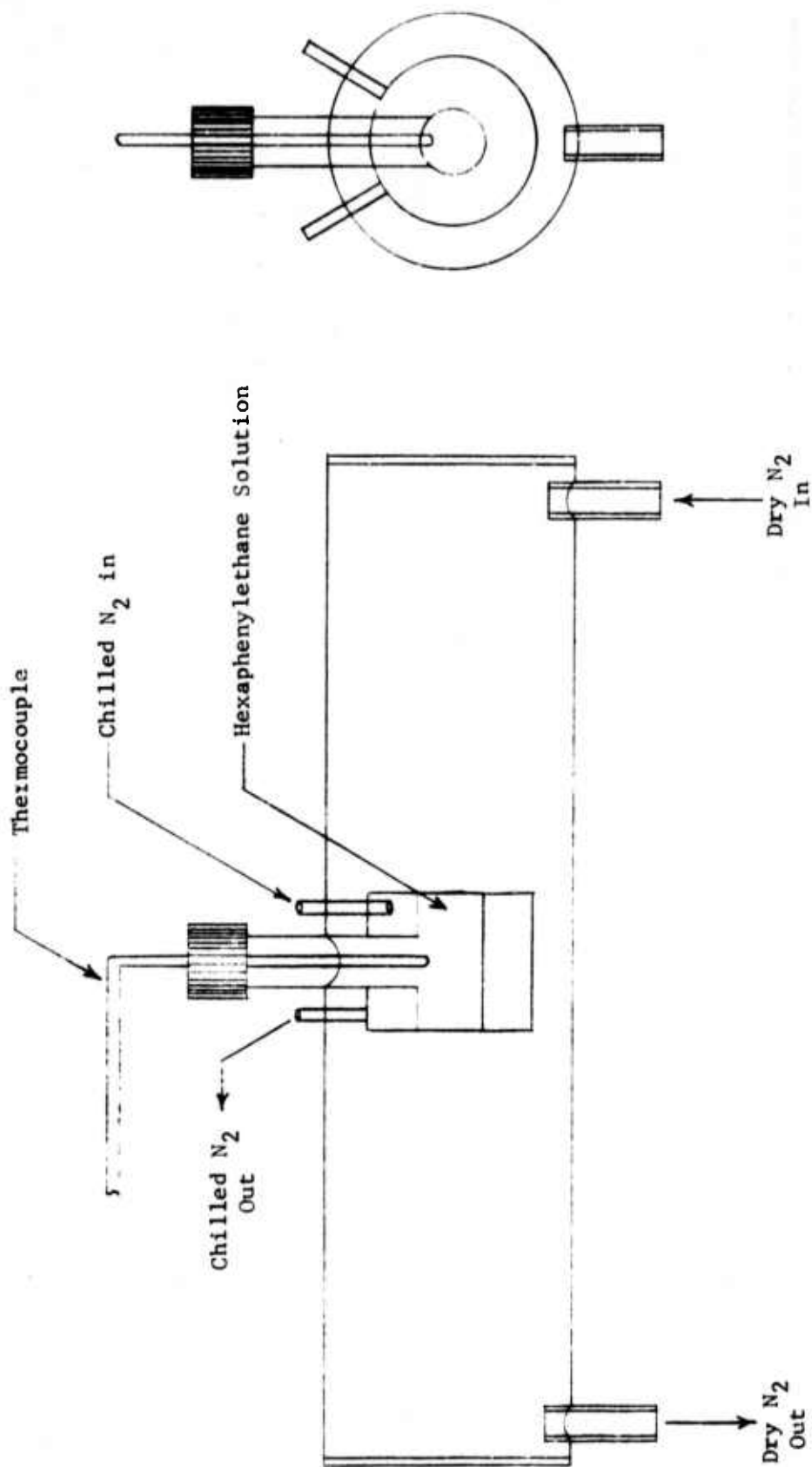


Figure 10. Schematic Diagram of Low Temperature Fluorescence Cell.

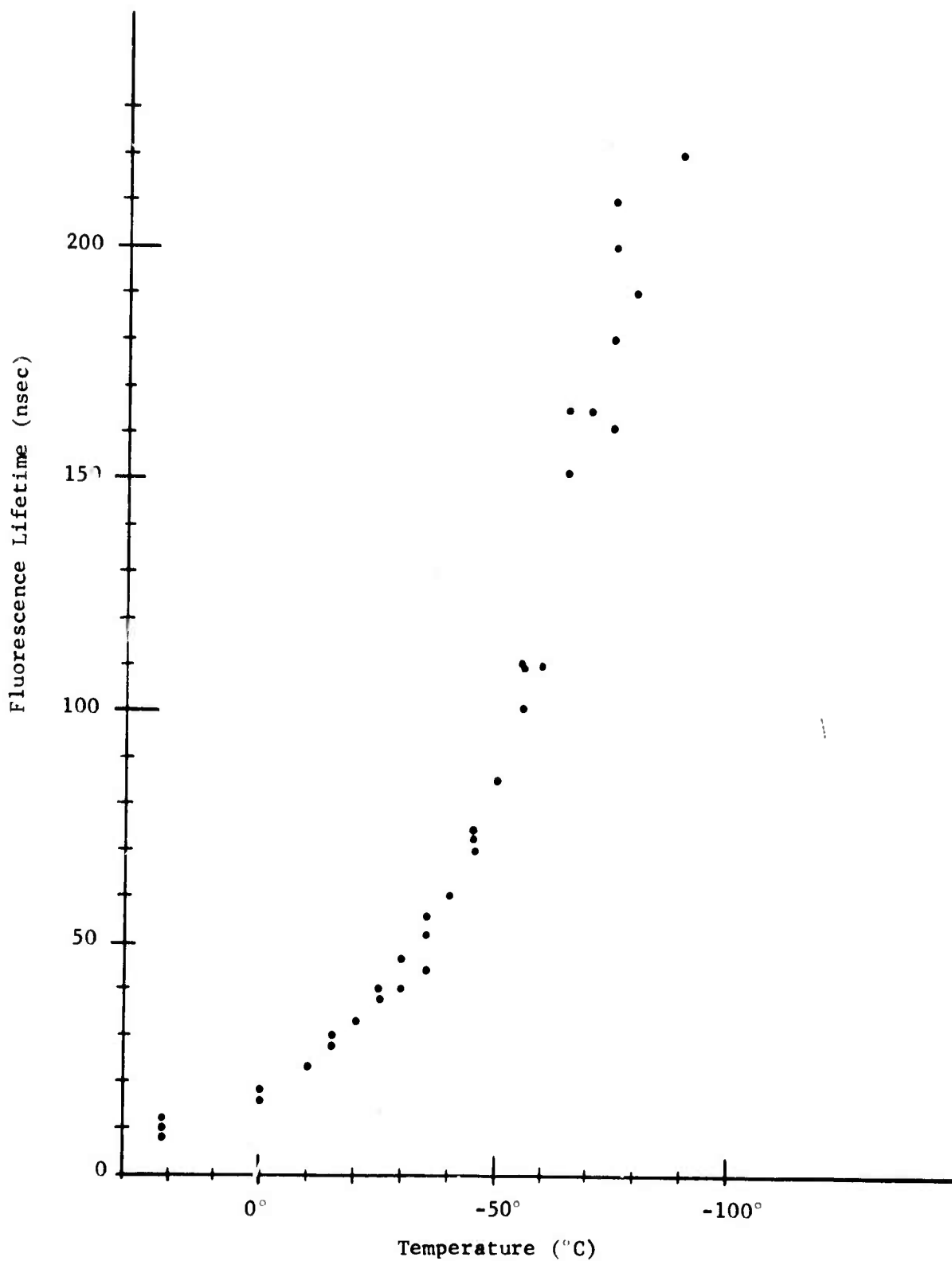


Figure 11. Temperature Dependence of the Triphenylmethyl Radical Lifetime. (Excitation Wavelength is at 5150 Å).

This dramatic increase in the fluorescence lifetime results from a decrease in the non-radiative rate constant k_{nr} . This non-radiative rate is due to a combination of internal conversion processes and deactivation of the excited level by solvent molecules, and it is reasonable to expect that both such effects exhibit a temperature dependence which acts to decrease the corresponding rate constants with decreasing temperature. Presumably if the temperature of the hexaphenylthane system is lowered even more, the fluorescence lifetime will approach the values reported by Okamura et al. (6) at -190°C . Since the solvent we used (iso-octane) turns into an opaque white solid upon freezing, we could not acquire data at any lower temperatures.

From the laser viewpoint, a longer fluorescence lifetime of the upper level would allow more energy storage in the medium. Better coupling of flashlamp sources would also be possible. In order to achieve this with hexaphenylethane as the active medium, the liquid would have to be cooled. Although this is undesirable, one could operate such a system at -78°C , achieved by a dry ice jacket around the active media. At this temperature, the fluorescence lifetime of the upper laser level would be ~ 190 ns.

(2) Temperature Dependence of the Fluorescence Intensity

Using the same experimental set-up described above, the fluorescence intensities were monitored as a function of cell temperature after irradiation with a 5150 \AA dye laser pulse. At this wavelength only radical excitation is energetically possible. Typical results are shown in Figure 12. The radical fluorescence is observed to decrease by about a factor of three as the temperature is lowered to $\sim -30^{\circ}\text{C}$, but very little subsequent decrease is noted as the sample is slowly cooled to even lower temperatures.

If one treats the radical as a two state system, and assumes rate constants k_p and k_T , where k_p describes the excitation rate to the upper state

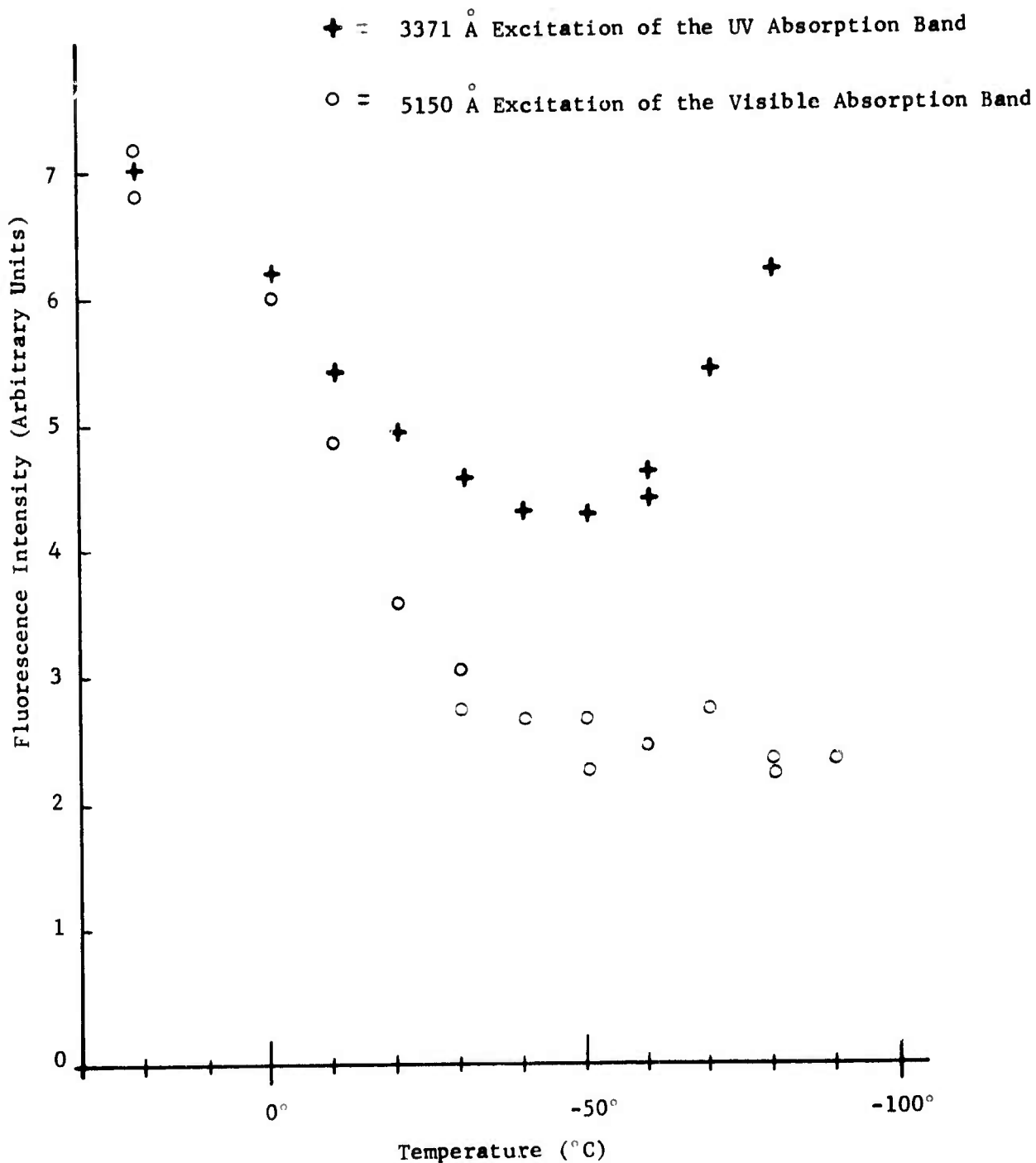


Figure 12. Temperature Dependence of the Triphenylmethyl Fluorescence Intensity Illustrating the Difference Between UV Excitation and Visible Excitation. The Fluorescence Intensities are Normalized to Each Other at Room Temperature.

and k_T the total decay rate back down to the ground state ($k_T = k_r + k_{nr}$), solution of the resulting rate equations gives the excited state population as a function of time. The peak of the fluorescence intensity (I) is then related to the rate constants and the initial ground state population density, $[R_0]$, by the expression

$$I \propto \frac{k_r k_p}{k_p + k_T} [R_0]$$

If the equilibrium constants reported in the literature are correct, the population density $[R_0]$ should decrease by about two orders of magnitude in going from room temperature to -90°C . The total decay rate k_T changes from $\sim 10^8$ at $+20^\circ\text{C}$ to $\sim 5 \times 10^6$ at -90°C . The pump rate under the experimental conditions is calculated to be $\sim 2 \times 10^7$. Using these values one can conclude that the fluorescence intensity should drop by a factor of twenty in going from room temperature to -90°C . Why a decrease of this magnitude is not observed experimentally is not clear. Perhaps the values cited in the literature for the equilibrium constants and/or the extinction coefficients are in error. Much of the experimental work to gather such data was performed more than 40 years ago, and significant experimental details are left out from many of the original references, making an evaluation of the accuracy of the data difficult.

b. Excitation of the UV Absorption Band

(1) Temperature Dependence of the Fluorescence Intensity

The hexaphenylethane-triphenylmethyl system is complicated by the fact that the dimer and radical exist at room temperature. As shown, the strong UV absorption of both the dimer and radical results in a broad absorption band which peaks at $\sim 3350 \text{ \AA}$. As a result, the fluorescence observed upon excitation

with a nitrogen laser (3371 Å) may be produced via two possible channels. The thermally generated radicals could be pumped directly to their second excited state, whereupon rapid internal conversion to the first excited state would result, with subsequent fluorescence to the ground state. On the other hand, upon absorbing the UV photon, hexaphenylethane could undergo photodissociation, producing excited state radicals which then fluoresce to the ground state. The PDL scheme relies on the latter channel as the production mechanism for the electronically excited radicals. In order to determine to what extent each of these channels contributes to the observed fluorescence, the temperature dependence of the fluorescence intensity was investigated. If the temperature could be lowered to the point where there is no appreciable thermal generation of triphenylmethyl radicals, any observed radical fluorescence would have to be due to dimers photodissociating into excited radical states. Unfortunately, the results of the last section indicate that even at the lowest experimental temperatures, fluorescence from thermally-generated radicals is still non-negligible.

Nevertheless, the presence of photodissociation-generated excited radical fluorescence can still be determined. If the observed fluorescence is due solely to the excitation of thermally generated radicals, then the choice of excitation wavelength should have no effect on the temperature dependence of the fluorescence intensity. Specifically, pumping the UV absorption band with the 3371 Å output of an N₂ laser should yield the same temperature dependence as seen when the visible absorption band of the radical is excited. However, if excitation in the UV causes, in addition to direct radical excitation, the photodissociation of hexaphenylethane dimers into excited state radicals, then the temperature dependence of the fluorescence intensity should be markedly different. This is because the dimer concentration increases with decreasing temperature (see Figure 4) and therefore the fluorescence intensity

due to a photodissociation process is expected to increase as well. On the other hand, the concentration of thermally generated radicals decreases with decreasing temperature, and, as has already been shown, so does the fluorescence intensity associated with direct excitation of these radicals. The experimental data shown in Figure 12 does show a distinct difference in the observed temperature dependence measurements, depending on whether only the radical is excited (pumping with 5150 Å) or whether both radical and dimer (pumping at 3371 Å) are excited.

The temperature dependence of the UV data can be understood by assuming that both direct excitation and photodissociation are involved in the fluorescence process. Initially the decrease in thermally generated radical population is the dominant factor, but at lower temperatures the photodissociation process becomes evident by the rise in fluorescence intensity. Unfortunately, because the pumping geometries and excitation volume were different in the two experiments it was not possible to obtain a quantitative contribution from each process to the fluorescence intensity. However, the data qualitatively supports the idea that UV absorption by the dimer causes photodissociation into excited state radicals.

(2) Temporal Behavior of the Fluorescence

Several important conclusions regarding the temporal behavior of the fluorescence decay can be drawn from the rate equation analysis outlined in Section IID. If only excitation of thermally generated radicals occurs, then the fluorescence should follow a single exponential decay: $I(t) = I_0 e^{-k_T t}$ where $k_T = k_r + k_{nr}$. This fact has been observed experimentally. However, when excited state photodissociation occurs as well, the fluorescence decay should be described by the sum of two exponentials: $I(t) = A e^{-k_T t} + B e^{-k_D t}$ where k_D describes the dissociation rate.

Analysis of the fluorescence decay curves produced by UV excitation, however, shows that the time dependence is still described by the single exponential decay $e^{-k_T t}$. For this to be consistent with the photodissociation concept, one must conclude that the k_D rate constant is very large. If $k_D > 10^9$, then for times greater than ~ 1 ns, the decay will be dominated by the first term and the second exponential would not be observable under our experimental conditions because of the response times of the phototubes and instrumentation.

c. Absolute Fluorescence Intensity Measurements

An absolute measurement of the room temperature triphenylmethyl fluorescence intensity was made by calibrating the observed fluorescence signals against the light output from a standard lamp of known brightness. The experimental procedure was as follows:

A known length of the fluorescence cell was transversely excited by the 3371 Å output of the N_2 laser. The fluorescence was focused onto the entrance slits of a monochromator and detected by a photomultiplier tube and fast oscilloscope. The sample was then replaced by a calibrated standard lamp, and the mechanically chopped output was focused by the same lens geometry onto the monochromator. Considerable care was taken to ensure that the collection geometry and solid angle filling factors were kept the same for both the fluorescence cell and the standard lamp. The wavelength at which the calibration was performed was 5200 Å, which corresponds to the peak of the triphenylmethyl fluorescence. By taking into account the appropriate geometrical factors, a value for the excited state population density N , can be deduced from the measured intensities using the expression

$$N = \frac{4\pi \Delta\nu}{h\nu A\Omega\delta\nu} \frac{B_S}{I_S} I_f$$

where $\Delta\nu$ = bandwidth of fluorescence (taken to be $\sim 500 \text{ \AA}$)

$\delta\nu$ = acceptance bandwidth of the monochromator

l = excitation length (= 2 cm)

A = Einstein coefficient

B_s = known spectral lamp brightness in units of

$$\left(\frac{\text{power}}{\text{area-steradian-wavelength}} \right)$$

I_f, I_s = the resulting phototube current produced by the
fluorescence and standard lamp, respectively.

The results of these measurements show that a 200 kW, 8ns N_2 laser pulse produces $\sim 2 \times 10^{15}$ radicals/cc in the electronically excited state. Since $\sim 2 \times 10^{17}$ photons/cc are absorbed during each pulse the quantum yield for production of excited state radicals is $\sim .01$.

The fluorescence intensity was also observed to increase linearly with pump power, demonstrating that the excitation process is not multiphoton in character, and that possible absorption of the fluorescence by higher lying states is not significant.

If one assumes that the lower laser level is empty, then the excited state population density can be related to the maximum possible gain one can expect from this system. The gain coefficient $\alpha(\nu)$ can be written as

$$\text{The gain coefficient } \alpha(\nu) = \frac{c^2 AN}{8\pi \nu^2 \Delta\nu}$$

Using our calculated value for N , the above expression gives an upper bound value of $.02 \text{ cm}^{-1}$ for the gain coefficient at the peak of the triphenylmethyl fluorescence curve, under our experimental conditions.

d. Fluorescence Intensity as a Function of Excitation Wavelength

This study was motivated by the fact that although the peak of the hexaphenylethane-triphenylmethyl UV absorption curve lies very close to the 3371 Å nitrogen laser wavelength, the cross section for photodissociation into excited state radicals may peak at a different wavelength, and as a result, larger fluorescence yields may be obtainable at other wavelengths even though the UV absorption is less. In addition, a knowledge of how the triphenylmethyl radical fluorescence intensity varies as a function of excitation wavelength is necessary in order to make an evaluation of different possible pumping mechanisms (e.g., laser vs flash-lamp).

A frequency-doubled dye laser was used to provide a tunable UV source for these measurements. The peak of the fluorescent emission (5200 Å) from the hexaphenylethane solution was passed through a monochromator and detected by a 1P21 photomultiplier tube. The pulsed output was time-averaged with a PAR 160 boxcar integrator. A Molelectron J3-05 joulemeter was used to measure the incident laser intensity at each wavelength. Figure 13 shows the results of this series of measurements. The plotted ratio represents the hexaphenylethane fluorescence intensity normalized to the incident excitation intensity. If a comparison of this curve to the hexaphenylethane UV absorption curve (Figure 6) is made, one sees that they are quite similar in shape.

From the point of view of assessing an appropriate optical pump source for hexaphenylethane, these findings lead to some important conclusions. Optical pumping by a N₂ laser looks attractive for two reasons. First of all, the N₂ laser output of 3371 Å falls close to

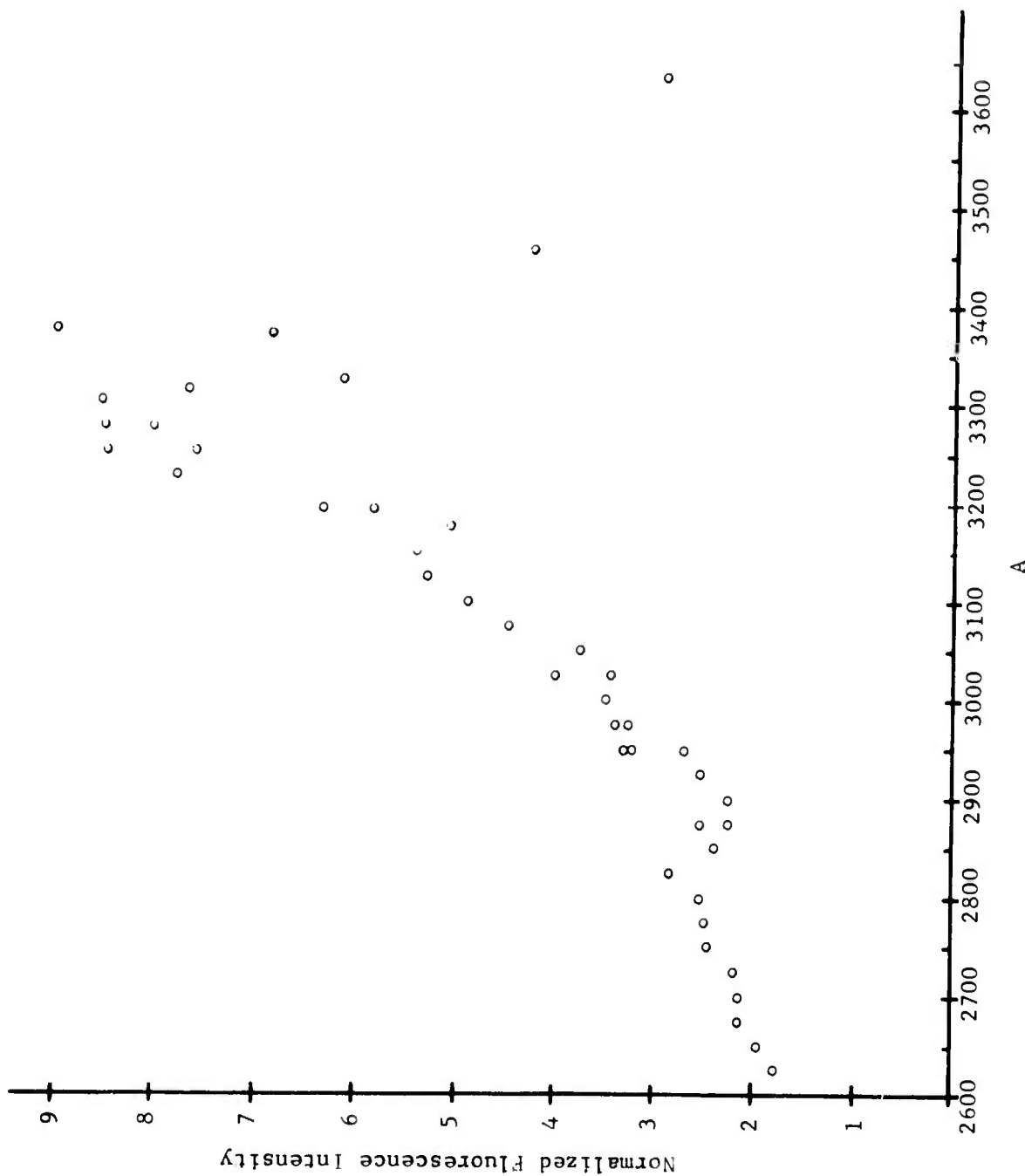


Figure 13. Hexaphenylethane fluorescence intensity plotted as a function of excitation wavelength. The fluorescence intensity shown is normalized to the incident intensity at each wavelength.

the peak of the UV absorption curve. Secondly, optical pumping at this wavelength not only results in the maximum absorption, but in the largest fluorescence quantum yield as well.

An attempt at achieving laser action in a solution of hexaphenylethane in isooctane was made utilizing N_2 laser pumping. The 300 kw, 8 ns output of our N_2 laser was focused onto a quartz cell equipped with Brewster angle windows. Two highly reflective dielectric coated mirrors served to form a resonant cavity. However, no laser action was observed from this configuration. Unfortunately, the excitation length one can achieve with the N_2 laser for a given power density is essentially limited by the beam geometry. In our case, using a cylindrical lens to form a line image, the effective excitation length is ~ 2.5 cm.

Taking our estimated value for the gain coefficient of $.02 \text{ cm}^{-1}$, this means that the single pass gain through the hexaphenylethane solution is at most 5%, and this is not sufficient to overcome other cavity losses.

Xenon flashlamp pumping has been considered as a means of exciting a longer excitation length. In the N_2 laser pumping experiment, $\sim 10 \text{ MW/cc}$ are absorbed by the hexaphenylethane solution. In order to maintain this absorbed power density along a 15 cm length of active region would require a flashlamp output power equivalent to $\sim 2 \text{ MW}$ at 3371 \AA . The fact that the flashlamp output is broadband and that both the hexaphenylethane absorption and triphenylmethyl radical fluorescence falls off rapidly as one moves further into the UV from 3371 \AA means that the flashlamp output must be on the order of $\sim 10 \text{ MW}$ in the range $2800\text{-}3600 \text{ \AA}$ in order to be equivalent to the N_2 laser pump in exciting the hexaphenylethane solution. These large pumping requirements have led us to the conclusion that Xenon flashlamp pumping of hexaphenylethane would be highly impractical.

e. Photochemical Stability

A serious problem in the use of hexaphenylethane as a laser medium is its photochemical stability. Figure 14 shows five successive measurements of fluorescence from a room temperature hexaphenylethane solution excited by a 200 kW N₂ laser pulse at a repetition rate of 3Hz. Initially, the fluorescence spectrum is dominated by the characteristic triphenylmethyl radical fluorescence. However, a broad peak centered at $\sim 4200 \text{ \AA}$ is also seen. Each scan took about 10 minutes to complete. The curves are labelled with their respective starting times. As can be readily seen, successive UV excitation results in a decrease of the triphenylmethyl fluorescence intensity and a growth in the intensity of the broad peak. After about half an hour of continuous excitation (5400 pulses), the triphenylmethyl fluorescence intensity is reduced to half its value. In less than an hour ($\sim 10,000$ pulses) the triphenylmethyl radical fluorescence has virtually disappeared and the fluorescence intensity is totally dominated by the peak in the blue spectral region.

This photochemical instability is the result of the irreversible disproportionation reaction discussed earlier (See Section IIB-1a). The blue fluorescence is attributed to the formation of 9-phenylfluorene, a by-product of the reaction. This reaction proceeds at an even faster rate when the sample is exposed to ordinary sunlight. Indications exist, however, that the photochemical stability is enhanced if the solution is cooled below room temperature. In solid matrices, hexaphenylethane does not exhibit this photosensitivity at all (9). This is due to the bimolecular nature of the process.

Excitation Wavelength: 3371 Å
Excitation Power: 200 kw/pulse @ 3 Hz Repetition Rate

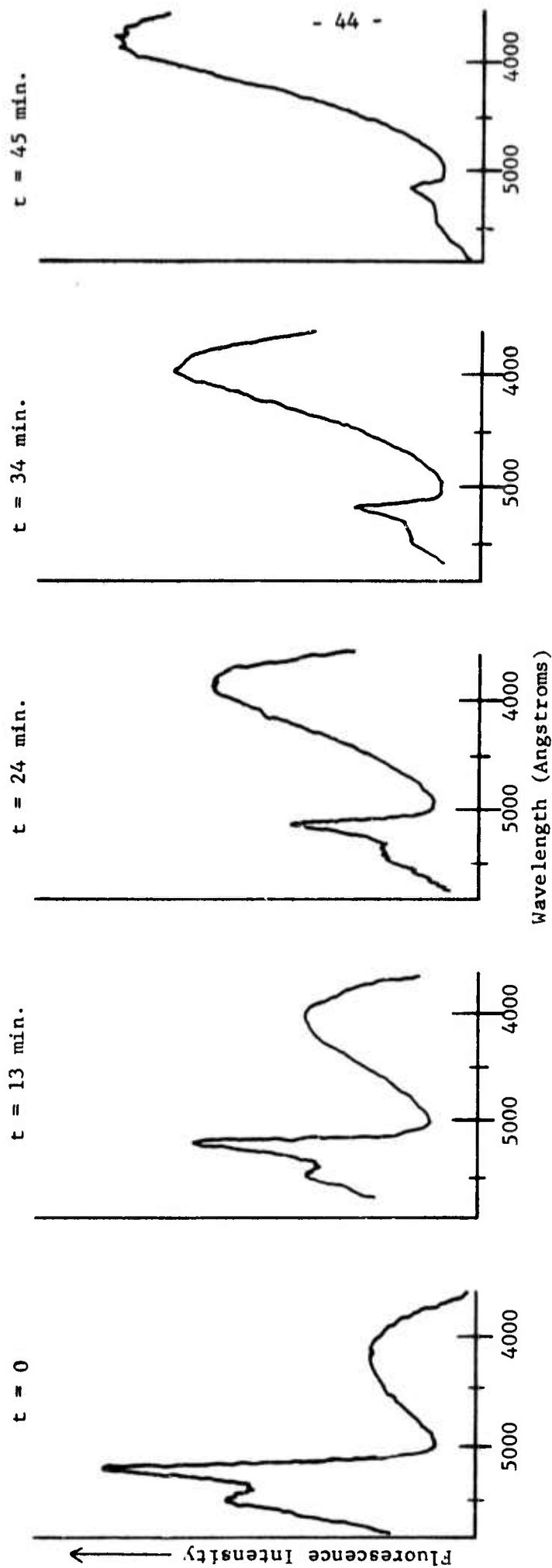


Figure 14. Successive Scans of the Hexaphenylethane Fluorescence Showing the Effect of the Disproportionation Reaction. The Triphenylmethyl Fluorescence Intensity Decreases With Time, and the Blue Fluorescence of one of the By-Products of the Reaction (9-phenylfluorene) is Seen to Increase.

2. Other PDL Molecules

In addition to the work on hexaphenylethane, fluorescence spectra were obtained for the other PDL molecules that were synthesized at the start of the program. The excitation source for all the spectra discussed below is a frequency doubled dye laser tuned to 2600 Å. All the molecules discussed below are strongly absorbing at this wavelength.

(a) Pentaphenylethane - Breaking of the central carbon-carbon bond results in the production of both triphenylmethyl and diphenylmethyl radicals. As mentioned previously thermal production of such radicals has been noted historically as color changes in heated solutions of pentaphenylethane. The fluorescence spectrum shown in Figure 15 does not show any features in the visible that can be associated with production of these radicals in an excited electronic state. Rather, a broad feature in the UV dominates the spectrum and is probably due to fluorescence of the pentaphenylethane dimer structure. We conclude that UV excitation of pentaphenylethane does not result in any significant photolytic production of electronically excited radicals.

(b) 1-p-biphenyl-1,1,2,2-tetraphenylethane - For this molecule as well, thermal dissociation into radicals has been observed by noting that clear solutions turn colored upon heating due to the visible absorption spectrum of the radicals. However, the fluorescence spectrum we have taken (Figure 16) does not show any corresponding visible fluorescence that would be indicative of the formation of radicals in an electronically excited state. The weak fluorescence that is observed in the UV can be attributed to the dimer.

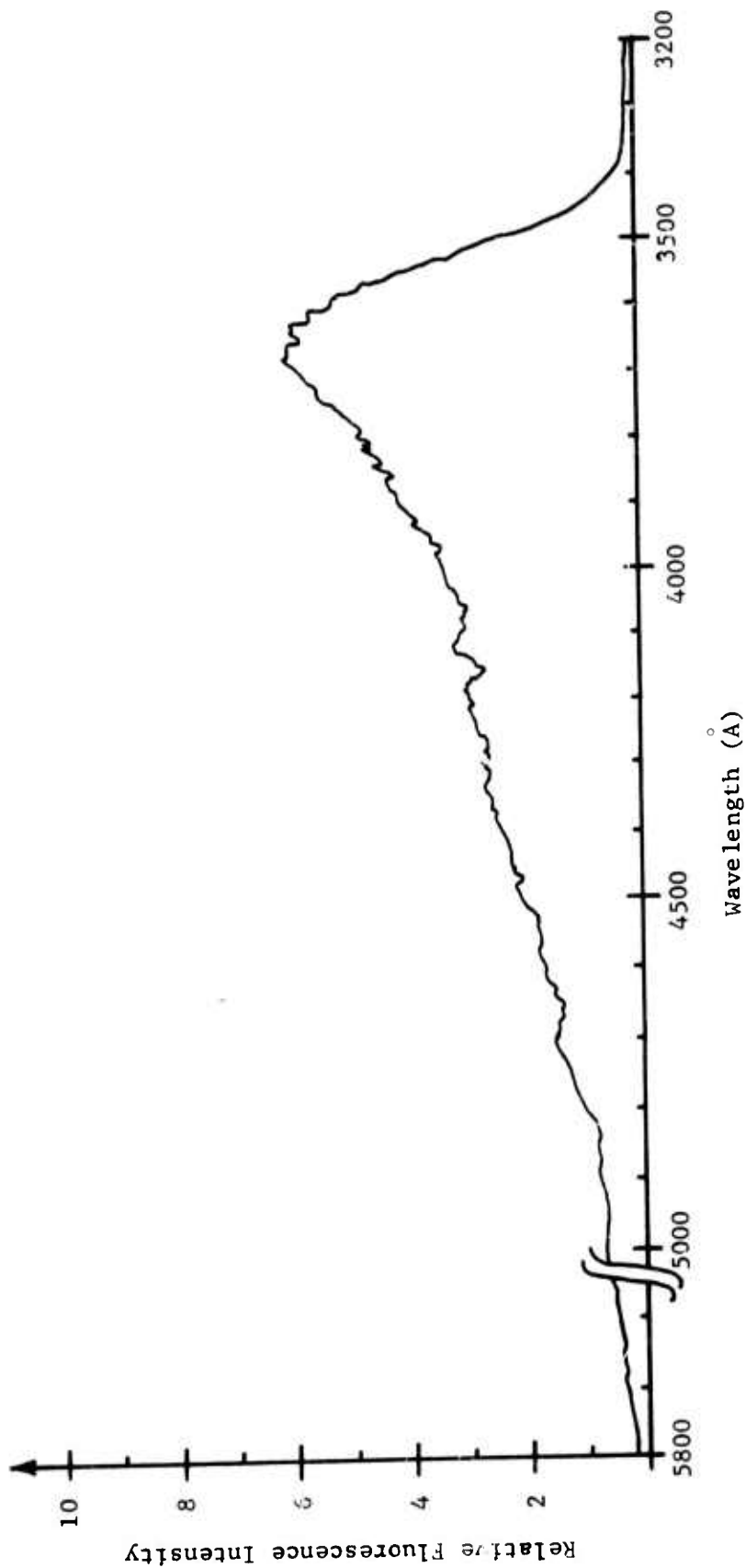


Figure 15. Fluorescence Spectrum of pentaphenylmethane. The excitation source is a frequency doubled dye laser operating at 2600 Å.

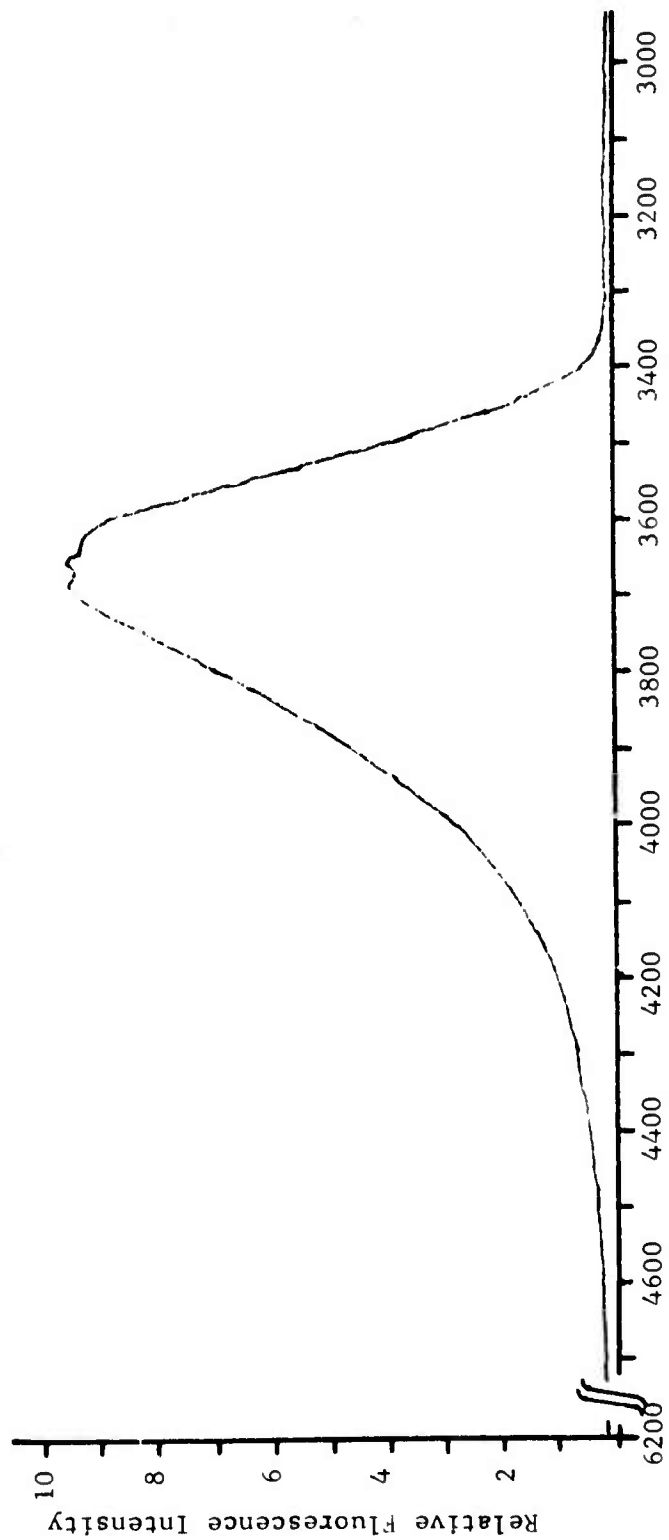
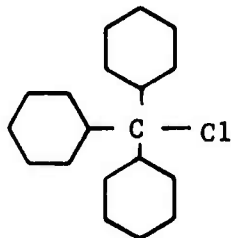


Figure 16. Fluorescence Spectrum of 1-p-biphenyl-1,1,2,2 tetraphenylethane excited by a frequency doubled dye laser operating at 2600 Å.

(c) 12-12' Bifluoradenyl - No evidence for thermal dissociation into radicals has been reported in the literature for this structure. The fluorescence spectra we have observed (Figure 17) indicate several peaks in the blue and UV. However, the fluorescence intensity is extremely weak.

The fluorescence lifetime of all these molecules has been measured. The room temperature lifetimes are all ~10 ns with no observable change as the temperature of the medium is lowered to ~-100°C.

(d) We have also investigated one molecule that was not one of the original PDL molecules synthesized at the start of the program. This molecule is triphenylmethylchloride:



Irradiation of a solution containing this molecule with 2600 Å light results in triphenylmethyl radical fluorescence. Photodissociation resulting in excited radical states is clearly seen to occur in this material. However, the fluorescence quantum yield is less than 1%, and therefore this molecule is not suitable as a PDL active media.

(e) Sesquixanthryl - This molecule could not be studied because of its insolubility in any compatible UV transmitting solvent.

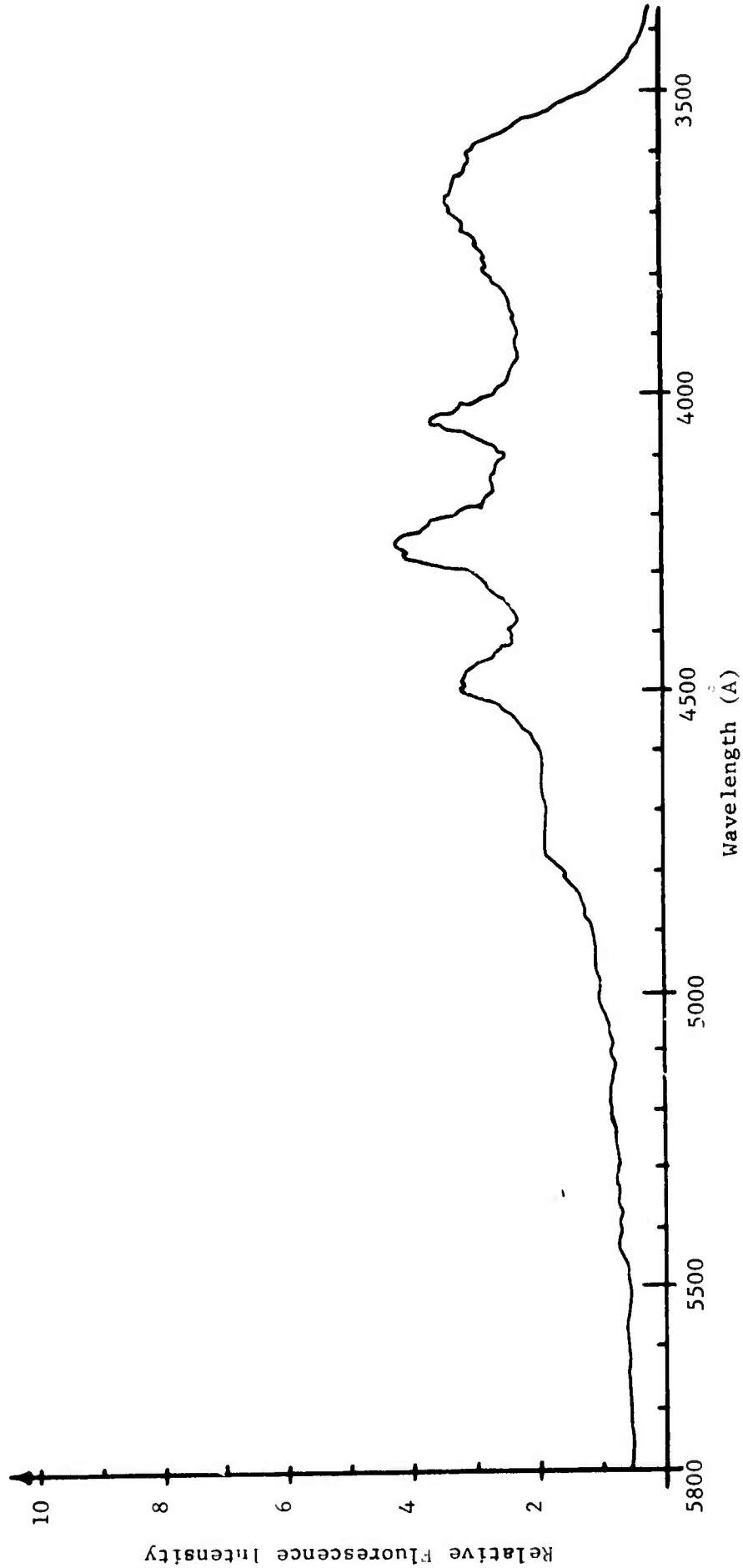


Figure 17. Fluorescence Spectrum of 12-12'bisfluoradenyl excited by a frequency doubled dye laser operating at 2600 A.

F. Conclusions

The five hexaarylethanes synthesized at the start of the program have been investigated for their potential use as active media for a laser operating under the PDL scheme described in Section IIA.

The most promising molecule of the group appeared to be hexaphenylethane. Photodissociation of the dimer into excited state triphenylmethyl radicals was observed and long fluorescence lifetimes (200 nsec) have been measured. However, these long lifetimes are observed only at low temperature (-80°C). On the basis of absolute fluorescence intensity measurements, potential optical gains of $.02 \text{ cm}^{-1}$ were calculated at the peak of the fluorescence band (5200 \AA), assuming no ground state population.

Fluorescence intensity measurements as a function of excitation wavelength indicated that the optimum optical pump source for the hexaphenylethane system is the N_2 laser. However, because the maximum gain for this system is expected to be low, the length of active media that can be excited by a N_2 laser is too short to overcome single pass cavity losses. Experiments to achieve laser action in this system proved unsuccessful. Chemical reactivity problems associated with hexaphenylethane were also investigated.

Of the four remaining hexaarylethane molecules, one, sesquianthryl, could not be considered because it proved to be insoluble in any UV transmitting solvents. The other three, did not exhibit photodissociation into excited state radicals upon UV excitation.

We conclude, therefore, that the hexaarylethanes that we have investigated in this program are not suitable as laser media for a PDL

system. Furthermore, continued work to investigate the viability of the PDL concept will necessitate the investigation of other groups of organic molecules that look promising. Possible choices of consider for such an investigation are the dilactones, the aloxytetraarylethanes, and tetraphenylallyl molecules, since all these groups have been reported to reversibly dissociate into radicals.

III. HIGH PRESSURE DISCHARGE CONDITIONING STUDIES

Towards the end of March 1976, sufficient data had been obtained on the existing PDL candidates to conclude that the hexaarylethanes as a group did not hold promise as PDL laser media, and that a lengthy synthesis program was required to prepare other promising organic molecules for further study. Such a synthesis effort would have required several months work, with little time left in the program for an evaluation of the synthesized materials. The PDL effort was therefore concluded at the end of March, and, as a result of a contract modification, a six month effort initiated to investigate a new high pressure discharge technique. Specifically, the primary objective of the new program was the investigation of the applicability of thermionic emission to sustain a spatially uniform discharge in a high pressure gas.

A. Background

The development of efficient, practical, high energy visible gas lasers is limited, in large measure, by the techniques presently available for the excitation of the laser medium. Uniform excitation must be provided to a large volume of the active medium which, in the most general case, consists of a gas or vapor at pressures in excess of one atmosphere and possibly at elevated temperatures.

Three excitation techniques are presently available for high pressure laser media. These are (a) the self-sustained discharge, in which both the density of electrons and the optimum average energy required for excitation are obtained through breakdown of the laser medium; (b) the externally sustained discharge in which the electrons are provided by an external source such as uv photoionization or electron beam injection while

the optimum average electron energy is independently maintained by an electric field; and (c) the excitation by thermalized secondary electrons generated from ion pair production by high energy electron beams.

The externally sustained discharge provides, in principle, the greatest control over the optimization of the plasma parameters relevant to the excitation of the laser levels. In practice, the advantages of this technique have been dramatically demonstrated in CO₂ lasers, and several rare gas-halogen systems. The applicability of the scheme to high energy visible lasers depends on the characteristics of the specific system; that is, the cross-sections for excitation and ionization as well as the energies of the upper laser level and the ionization continuum.

Independent of whether or not the excitation can be provided by a self-sustained or externally sustained discharge, the general problem with high pressure media is the tendency of the discharge to evolve into constricted regions due to the reduction, at high pressure, in the diffusion of the electrons which constitute the primary avalanches. If the space charge developed by the growing primary avalanches severely distorts the applied electric field, localized regions of high conductivity, called streamers, develop which lead to arc breakdown.

In an attempt to overcome these problems in the case of self-sustained discharge excitation, conditioning of the laser medium by low energy discharge and uv photoionization has been applied, with some success, to atmospheric HF and CO₂ lasers. However, these techniques are relatively inefficient and produce low density, spatially non-uniform pre-ionization. They are not directly applicable to large volume, multi-atmosphere visible gas laser media.

In the case of uv sustained discharge excitation, pre-ionization has been generated by the photoionization of organic species, with low ionization potentials, seeded in the laser medium. Pre-ionization densities of 10^{12} electrons-cm⁻³ have been reported in atmospheric CO₂ lasers. This technique, however, is inefficient due to the small photoionization cross-sections.

Finally, techniques involving the use of electron beams, while eminently suited for demonstration and prototype lasers, suffer the disadvantages of inefficiency, complexity, large size and weight, and expense. High pressure laser media require very high energy electron beams due to the requirements of penetration through the electron window as well as the laser medium. Large volume lasers require large area guns with associated current uniformity problems.

Alternate techniques for the suitable excitation of high pressure media must clearly be developed if efficient, reliable, high energy, visible gas lasers are to be successfully integrated into practical systems.

B. Breakdown Mechanisms in High Pressure Gases and Vapors

In the absence of sufficient pre-ionization, electrical breakdown in gases and vapors where $pd \gtrsim 1000$ torr-cm usually occurs in narrow channels of extremely high conductivity. There are two breakdown mechanisms which have been proposed to explain such behavior. A brief description of these theories follows.

1. Townsend Breakdown

In this scheme, individual electron avalanches are initiated by free electrons that are produced either in the gas or at the electrode surface. These electrons gain energy in the applied field and lose energy

by collisions with the gas. Additional electrons produced from ionizing collisions participate in further ionization, thereby forming avalanches. The primary electron multiplication process is conventionally described by α , the first Townsend ionization coefficient (10). This coefficient is defined as the average number of ionizing collisions per centimeter of path made by electrons drifting in the direction of the applied field.

Assuming a plane parallel electrode geometry with spacing d where $n_e(x')$ is the initial electron density at position x' from the cathode, the increase in density dn_e can be written as:

$$dn_e = n_e(x')\alpha(x')dx'$$

Integration of this equation shows that the number of electrons in an avalanche increases as

$$n_e(x) = n_e(0) \exp \left[\int_0^x \alpha(x')dx' \right] \quad (1)$$

In general, $\alpha(x)$ depends on the electric field and pressure.

In one transit time, the current i_0 , which would have been collected in the absence of ionization is increased to $i_0 \exp \left[\int \alpha(x)dx \right]$, where the number of electrons M , created by the avalanche process is:

$$M = \exp \left[\int \alpha(x)dx \right] - 1 \quad (2)$$

Experimentally, the current in a discharge is seen to rise faster than exponentially as a result of secondary ionization effects. The Townsend theory invokes the creation of δM new electrons by such secondary processes, where δ is called the second Townsend coefficient. These secondary processes include absorption of resonance and collisionally-induced photons by neutral species as well as collisional processes between ions and metastables. The electron density can then be shown to grow in the following manner:

$$n = n_0 \frac{\exp \left[\int \alpha(x) dx \right]}{[1-\gamma M]} \quad (3)$$

The relationship $\gamma M \approx 1$ represents the threshold condition for a self-sustained discharge. When this condition is satisfied, the avalanche process is essentially independent of the initial electron density.

2. Streamer Breakdown

Historically, the process which was claimed to contribute to the emission of secondary avalanches under the Townsend mechanism was the bombardment of the cathode by positive ions. However, experiments indicated that the breakdown times were much shorter than those allowed by the ion drift velocities. Loeb (11) and Raether (12) independently proposed "streamer" theories to replace the Townsend mechanism. The theories describe the attainment of breakdown as the evolution of a discharge channel of high conductivity (streamer) from the single primary Townsend avalanche, in the following manner:

The applied electric field is distorted by the build-up of the electron density in the head of the primary avalanche. The action of this space charge produces a local intensification of the electric field. Photons produced in the vicinity of the avalanche lead to photoionization. The electrons formed from this photoionization then produce secondary avalanches which feed into the primary avalanche. The transition from an electron avalanche into a streamer is considered to occur when the space charge field produced by the electrons at the head of the avalanche is comparable in magnitude to the applied field. The streamer breakdown condition is obtained simply by equating the value of the applied field to the space charge field.

This results in an expression of the following form:

$$\alpha d_{\text{crit}} = \ln (4\pi\epsilon_0 E\lambda/e) + \ln d_{\text{crit}} \quad (4)$$

where d_{crit} is the critical distance an individual avalanche must propagate to initiate streamer breakdown (13). The first term is insensitive to gas parameters and is ~ 20 in mks units for typical discharge conditions. Hence, we have

$$\alpha d_{\text{crit}} = 20 + \ln d_{\text{crit}} \quad (5)$$

as the discharge criteria under the streamer theory.

3. Considerations Affecting Spatial Uniformity

The spatial growth of ionization is determined by the drift velocity in the direction of the field and by the action of diffusion transverse to the field. As the ionization increases along the field direction, spatial separation of the electrons and positive ions occur due to their different drift velocities. The electrons form the head of the avalanche. The radial extent of the avalanche is determined by diffusion. This is illustrated in Figure 18. It can be shown that the average distance ρ , from the avalanche axis, at a distance x from the cathode is given by $\rho(x) = \left(\frac{2\lambda}{3} x\right)^{\frac{1}{2}}$ where λ is the electron mean free path. The value of ρ corresponds to the distance at which the number of electrons has fallen to e^{-1} of its value on the avalanche axis.

Thus, the avalanche is essentially cone-shaped. As the pressure increases, the mean free path and hence $\rho(x)$ decreases. At high pressure, the avalanche becomes constricted and the current density increases, resulting in an increase in the neutral gas temperature. The increased temperature lowers the local neutral density, resulting in an increased value of E/n which leads to increased ionization. This instability culminates in an arc discharge.

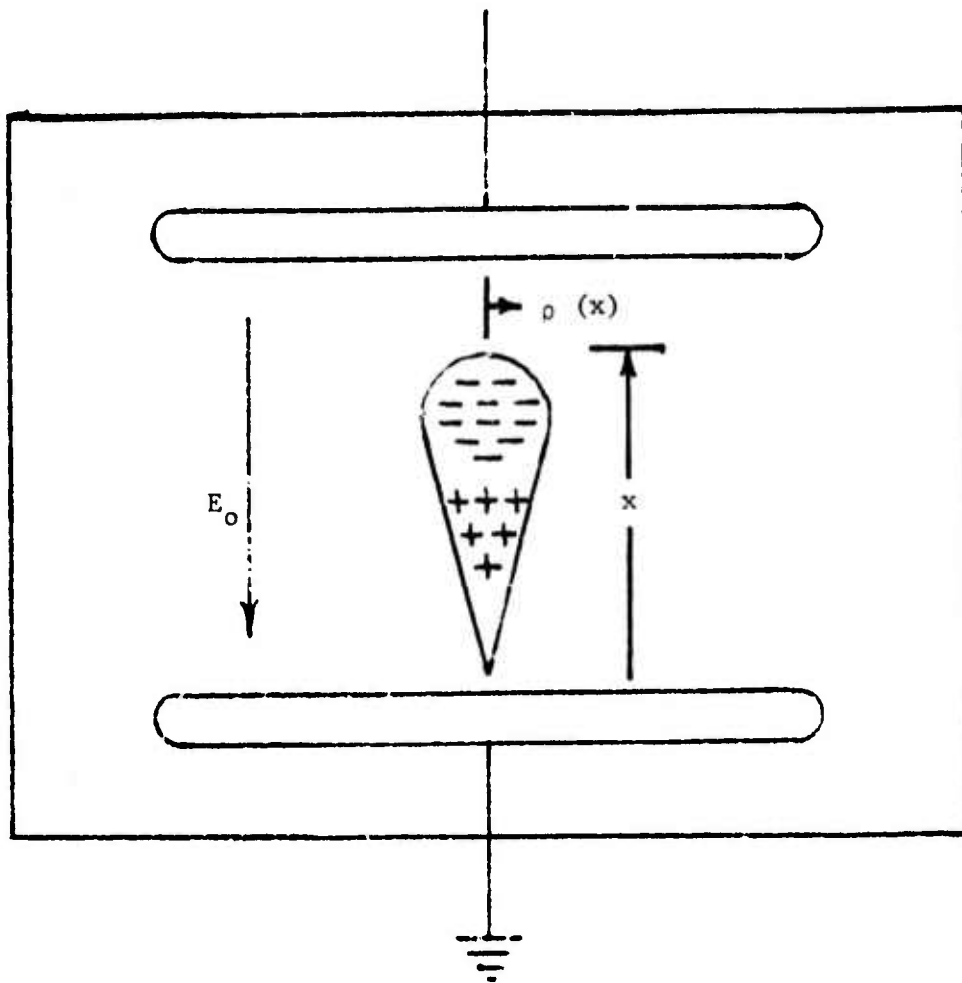


Figure 18: Spatial development of a Primary Electron Avalanche. The avalanche expands transverse to the applied field direction as it proceeds towards the anode due to diffusion. The quantity, $\rho(x)$, corresponds to the distance at which the number of electrons has fallen to e^{-1} of its value on the avalanche axis and is proportional to $x^{\frac{1}{2}}$.

From the above considerations, one can conclude that a necessary condition for producing uniform breakdown over large area electrodes is that the number of primary avalanches per unit area at the cathode surface must be sufficiently large so that spatial overlap of adjacent avalanches occurs before electric field gradients are allowed to develop which will lead to field distortion.

Quantitatively, this condition implies that the electron density be sufficiently high such that at least one electron per "diffusion volume" is produced. This volume may be conservatively defined to be a sphere with radius equal to one mean free path. Consequently, we require

$$n_e \geq \frac{3}{4\pi\lambda^3} \geq \frac{1}{2} (\sigma n_0)^3 \quad (6)$$

The minimum gas density of interest here is one atmosphere or $3 \times 10^{19} \text{ cm}^{-3}$.

If the excitation cross section is assumed to be $5 \times 10^{-16} \text{ cm}^2$, then the minimum required density at the cathode is:

$$n_{e/\text{min}} \approx 8 \times 10^{11} \text{ cm}^{-3}$$

Another aspect which pertains to the generation of spatially uniform discharges is related to the statistical nature of the breakdown process. A parameter which is of particular importance is the statistical time lag, τ_s , which represents the average time interval between the liberation of electrons which initiate adjacent primary discharges. Loeb (13) has shown that this time lag can be written as a function of the initial number of electrons and the applied voltage.

$$\tau_s (i_0, V) = \left[\frac{i_0}{e} P_0(V) \right]^{-1} \quad (7)$$

where $P_0(V)$ is the probability that a single avalanche will lead to breakdown for an applied voltage, V .

Wisjman (14) has shown that the probability $P(i_0, V, \tau)$, that breakdown will occur for an applied uniform voltage, V , in a time interval τ following the application of the voltage may be expressed as:

$$P(i_0, V, \tau) = 1 - \exp \left\{ - \left(\frac{i_0}{e} \right) P_0(V) (\tau - \tau_F(V)) \right\} \quad (8)$$

where τ_F is the formative lag time. This is just the time required for the current to reach e^{20} times the initial value, namely:

$$\tau_F \approx 20 (\alpha v_d)^{-1} \quad (9)$$

Equation 8 then becomes:

$$P(i_0, V, \tau) = 1 - \exp \left\{ - (\tau - \tau_F) \tau_s^{-1} \right\} \quad (10)$$

In order to insure uniform breakdown over the entire electrode area, the statistical time must be made substantially less than the formation time.

$$\tau_B \ll \tau_F$$

From equations 7 and 9 we can write:

$$\left[\frac{i_0}{e} P_0(V) \right]^{-1} \ll 20 (\alpha v_d)^{-1} \quad (11)$$

If the voltage is such that the breakdown probability is ~ 1 , then $i_0/e \gg \alpha v_d/20$. For 1 atmosphere, $\alpha v_d \approx 10^7 \text{ sec}^{-1}$. This implies that the production rate of electrons must be greater than $\sim 10^6/\text{sec}$.

To summarize, the above arguments indicate that two criteria must be satisfied to ensure uniform discharges at a given pressure. The electron density at the cathode surface must be sufficiently high so that spatial overlap of the avalanche cones occurs before space charge field distortion effects begin to dominate. In addition, the electrons must be produced quickly enough so that the statistical time lag is less than the discharge formative time.

The work described in the following sections investigates the possibility of using thermionic emission at the cathode surface as a technique for meeting these criteria and thereby allowing for the generation of uniform discharges at pd values ≈ 1000 torr-cm.

C. Predischarge Conditioning by Thermionic Emission

The emission of electrons from a heated metal surface results in an electron density n_e , at the surface which may be shown to be given by:

$$\begin{aligned} n_e &\approx 2(2\pi m_e kT/h^2)^{3/2} \exp[-\phi/kT] \\ &\approx 5 \times 10^{15} T^{3/2} \exp[-\phi/kT] \text{ cm}^{-3} \end{aligned} \quad (12)$$

where ϕ is the work function and T the absolute temperature of the electrode material. A more familiar expression, Richardson's equation, expressing the current density j_o , may be obtained from the above equation by multiplying the expression for n_e by ev_{thermal} , resulting in

$$j_o \approx 120 T^2 \exp[-\phi/kT] \text{ amps - cm}^{-2} \quad (13)$$

These expressions are valid under the assumption that the applied field is large enough to extract all the electrons from the vicinity of the cathode so that a significant negative space charge field is not allowed to develop. Otherwise, this field serves to drastically reduce the number of emitted electrons to values far below those predicted by the above equation. The extent to which this condition is satisfied under our experimental conditions will be discussed later.

If the above assumption is satisfied, large densities of electrons can be generated at the cathode surface. For example, a pure tungsten emitter with ~ 4.5 eV work function can provide electron densities of $\sim 10^{12}$ cm^{-3} at temperatures of $\sim 2600^\circ\text{K}$. Similar electron densities may be obtained at significantly lower temperatures by using materials

having lower work functions than tungsten. Under such conditions, therefore, thermionic emission should not only be able, in principle, to provide sufficient pre-discharge conditioning to meet the uniform discharge criteria outlined above, but in addition, provide sufficient electron density to sustain the discharge with relatively little volumetric Townsend ionization.

D. Experimental Effort and Results

The initial direction of the experimental effort was dictated by several preliminary considerations. Firstly, one would like to construct a thermionic cathode from materials having as low a work function as possible so that the operating temperature is kept at a minimum. However, composite materials with low work function, such as various types of oxide-coated cathodes, lanthanum hexaboride, etc., are known to be extremely sensitive to positive ion bombardment, and as a result may not be able to structurally withstand a discharge environment. In order to avoid such complications, the applicability of these cathodes was not investigated during this preliminary "proof of principle" study.

If one considers the pure elements, only carbon and the refractory metals are sufficiently non-volatile at the temperatures required for appreciable thermionic emission. Unfortunately, these materials have work function of $\sim 4-4.5$ volts. The cathode materials investigated during this study consisted of tungsten, niobium, and graphite.

Secondly, it is clear that continuous thermionic emission for pre-pulse conditioning of high pressure laser media is neither desirable nor necessary. Rather, it is advantageous from several viewpoints to have the cathode heated for as short a time as possible prior to the electrical discharge pulse. In this manner, the average power necessary to maintain the electrode surface temperature is minimized, as are bulk gas and discharge structure heating effects.

Rapid pulse heating necessitates that the cathode mass be kept to a minimum. Consequently, the cathodes used in these studies were constructed from thin foils and meshes of the respective materials.

Two methods of rapidly heating thin sections of cathode materials to high temperatures have been investigated. The first method investigated the possibility of heating by discharging a high energy storage capacitor through the cathode elements. Both tungsten and graphite wires and foils were studied. In all cases, attempts at pulse heating these materials via capacitive discharge to temperatures of $\sim 2000^{\circ}\text{C}$ resulted in structural damage and eventual breakup of the material after several pulses. This resulted, presumably, from the inability of these materials to withstand the high peak currents that occur at the onset of the capacitor discharge.

The second technique investigated for rapid pulse heating of the cathode involves pulsed alternating current heating. In this technique, a high current variac is switched, within 8 msec, across the thermionic element. The current can be accurately switched on and off by an SCR controller. Such a controller allows the current on time to be controlled in steps of 8 msec ($\frac{1}{2}$ cycle). This technique was successful in repeatedly pulse heating tungsten and niobium foils to high peak temperatures ($> 2000^{\circ}\text{C}$) without the structural breakup problems associated with the capacitive discharge heating described above. Graphite foils, however, broke apart with this technique as well.

In order to test the thermionic discharge conditioning concept, an apparatus was designed which incorporates a pulse heated cathode into a transverse discharge geometry. A lucite structure acts as support and provides electrical insulation for the two electrodes. The aluminum anode has

a rounded Rogowski-like profile. The cathodes studied were made from 1 mil tungsten or niobium foil and various tungsten meshes of different mesh spacings. The heated cathode structure is depicted in Figure 19. As shown, the foil or mesh is flexed into an arch and then clamped along its length on either side for connection to the current feedthroughs. When the variac is pulsed on, current flow is in the direction shown. The cathodes studied were ~7 cm long with ~3 cm spacing between clamps. They were positioned 1.5-2 cm from the anode. A 30V high current variac was used to pulse heat these structures. Under our operating conditions, the 1 mil foils could be heated to ~2000°C in 100 msec. The meshes, because of their reduced mass, could be pulse heated to these temperatures in ~50 msec. Temperature measurements were made with a photodiode calibrated against an optical pyrometer using a dc heated element.

The electrical set-up used in these experiments is depicted in Figure 20. A pulse generator is used to trigger a back-to-back SCR (triac) switch. This acts to turn the variac on for a time determined by the time duration of the trigger pulse. When this pulse terminates therefore, the thermionic element is at its peak temperature. At this point in time, the trailing edge of the trigger pulse fires a thyatron which switches the discharge capacitor across the electrode gap. For our measurements, the discharge was triggered once every two seconds. At this low repetition rate, the discharge tube structure remained close to ambient temperature. Discharges were run at 760 torr pressure in He, Ar, and N₂, as well as admixtures of He with several percent SF₆. Discharge voltages up to 10 kV ($E/p = \sim 7.5 \text{ kV-cm}^{-1}\text{-atm}^{-1}$) were used for these experiments.

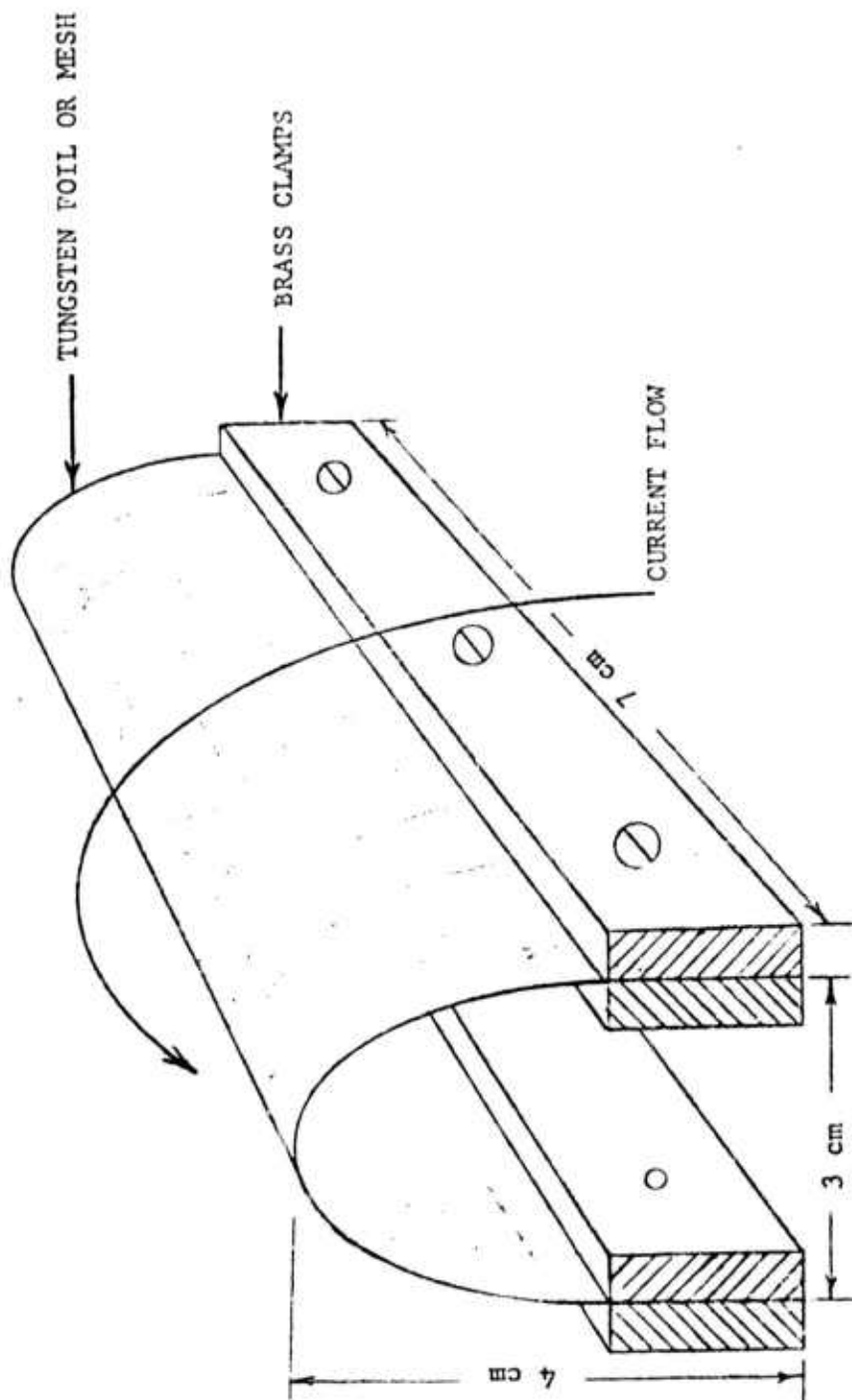


FIGURE 19: THE HEATED CATHODE STRUCTURE

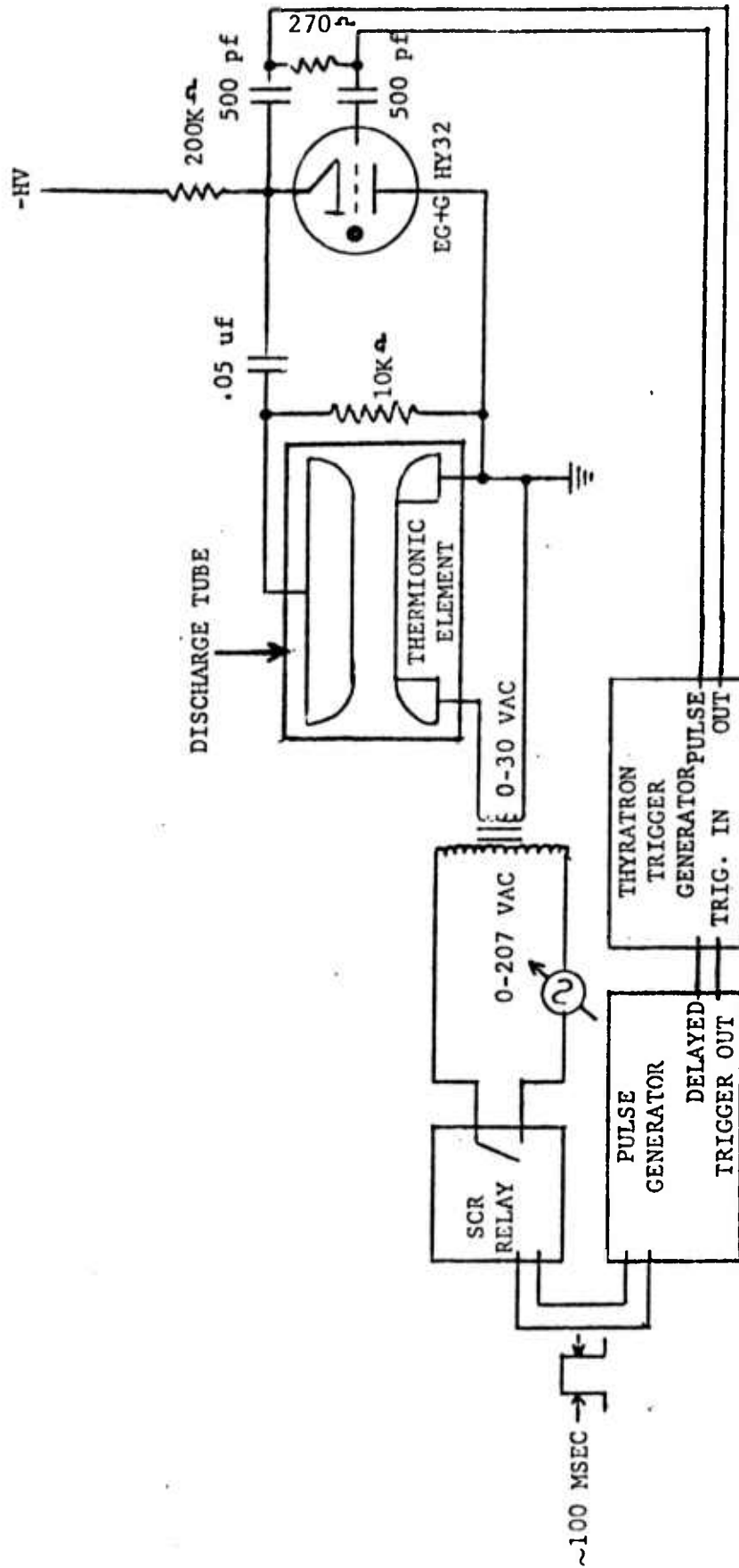


FIGURE 20: SCHEMATIC CIRCUIT FOR THERMIONIC ELEMENT DISCHARGE STUDIES

Qualitatively, the heated cathode effects on discharge uniformity were the same for all the gas mixtures that were investigated. In addition, no significant differences were observed between the use of niobium and tungsten as the cathode material.

Figure 21 illustrates what is observed at several different cathode temperatures, under operating conditions where self-sustained discharges were produced. The photographs show the discharge region and were taken through blue filters to cut down on the blackbody radiation emanating from the cathode, thereby making the discharge more visible. The cathode is visible in the lower part of the photographs as the luminous horizontal object. Also visible (especially in photograph #2) are two semicircular pyrex cylinders placed over the cathode at either end to shield the sharp edges of the foil or mesh from seeing a direct discharge path to the anode. The anode itself is visible in the upper half of the photographs by virtue of the reflected light from the cathode.

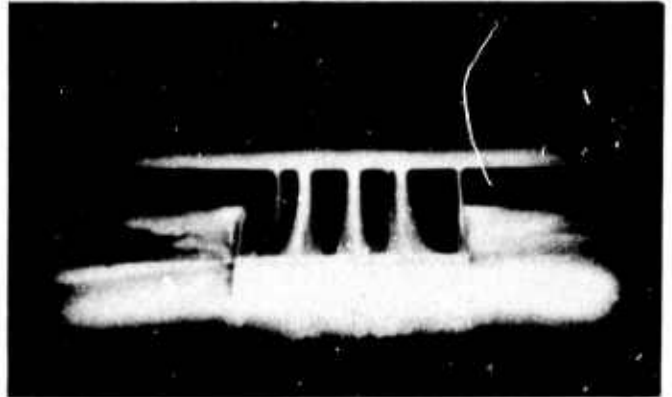
With the cathode at room temperature, the discharge constricts into an arc at one end of the discharge length. This is evident in photograph #1. As the cathode temperature is raised (photograph #2), multiple arcs begin to form, appearing flared out near the cathode surface. At a temperature of 1500°C (photograph #3), the entire discharge volume appears uniformly excited. Picture #4 is included for comparison of the blackbody intensity from the cathode under the same photographic conditions as picture #3, illustrating that the luminous volume between the electrodes in picture #3 is indeed due to discharge excitation, and not a spurious reflection off the back wall of the tube.

EFFECT OF THERMIONIC CATHODE ON DISCHARGE UNIFORMITY

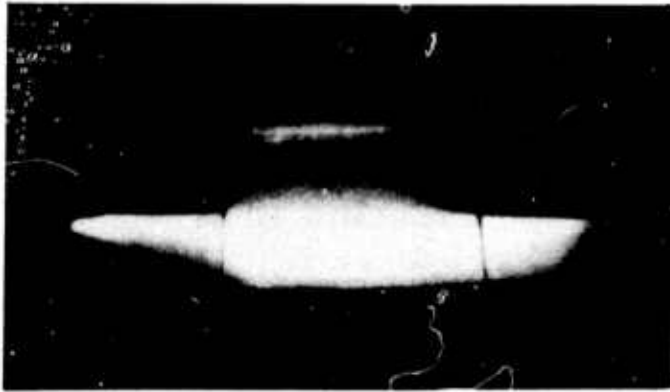
Experimental Conditions: Medium: Helium
Pressure: 760 Torr
Gap: 2 cm
Voltage: 10 kv



1. Discharge with cathode cold.



2. Discharge with cathode pulse heated to $\sim 1000^{\circ}\text{C}$.



3. Discharge with cathode pulse heated to $\sim 1500^{\circ}\text{C}$.



4. Cathode at 1500°C - no discharge.

Uniform discharges were obtained with both the foil and mesh structures. The advantage of using the mesh is that less energy is required to heat such a structure to the required temperature, compared with the foil, because of the reduction in mass. From an efficiency viewpoint, it is desirable to use as coarse a mesh as possible, made from wires with as small a diameter as possible. Typically, for the geometry used in these experiments, cathodes made from 100 mesh (100 wires per inch, cross woven with 100 wires per inch) of 1 mil diameter tungsten required ~90 joules of input energy to attain a pulsed peak temperature of ~1500°C. Meshes as coarse as 16 mesh (1/16" spacing between wires) tungsten were used and also resulted in uniform discharges. The extent to which the wire spacing can be increased beyond this value without affecting discharge uniformity was not investigated any further during this study.

Experiments were also carried out to determine the extent to which the discharge current could be sustained by the heated cathode. These measurements were made in 760 torr of helium and values of E/P of a few $\text{kV-cm}^{-1}\text{-atm}^{-1}$. Note that since only helium was used for these measurements, there was no stabilization of the ionization rate by attachment.

The peak temperature of the heated cathode was varied from 1500°C, at which point a uniform discharge was obtained, to 2300°C. It would be expected that if the discharge were sustained by the effects of the heated cathode, an increase in temperature for a fixed E/P would generate more electrons and reduce the plasma impedance. The discharge current should therefore increase and since the voltage is supplied by discharging a capacitor, the discharge rate should be faster (i.e., the pulse width shorter). This behaviour has been experimentally demonstrated. The discharge was spatially uniform and sustained by the thermionic element for 5 μsec

(limited by circuit capacitors). The peak current measured by a factor of two upon going from 1500°C to ~2400°C in cathode temperature. Concurrently, the pulse width was seen to decrease by the same factor, going from ~5 μ sec to 2.5 μ sec under these conditions.

E. Discussion of Results

Clearly, the temperature of the cathode has a profound effect on discharge uniformity. Let us consider this effect from the thermionic emission viewpoint. In the above experiments, cathode temperatures of ~1500°C were found to be sufficient to achieve a spatially uniform discharge at pd values in excess of 1000 torr-cm. At this temperature, the calculated electron density generated via thermionic emission at the cathode surface is (from equation 12) $\sim 10^8$ cm^{-3} . This value is calculated under the assumption of a 4.5 eV cathode work function. Such a density is considerably less than the 10^{12} cm^{-3} minimum density predicted to be necessary for a uniform discharge at 1 atmosphere from the considerations of section IIIB-3. However, it should be pointed out that the calculation of the minimum density in our treatment assumed that spatial overlap of the avalanche cones occurs within one electron mean free path from the cathode surface. If this condition is relaxed, the minimum required electron density decreases dramatically. For example, if we assume that overlap within 10 mean free paths is sufficient, then the required minimum density for a 1 atmosphere uniform discharge is reduced by 10^3 to $\sim 10^9$ cm^{-3} . Such a value is in reasonable agreement with that experimentally determined by us from a thermionic emission analysis. It should be pointed out that other theoretical treatments of the minimum electron density required to maintain uniform discharges at 1 atmosphere predict values as low as 10^4 cm^{-3} for some laser systems (15).

A further point to consider in more detail is the effect of space charge on the expected emission density under our operating conditions. As stated earlier, Richardson's equation, and the corresponding equation for the electron density (equation 12) are valid only if the applied field is large enough to assure that a space charge depression of the potential near the cathode does not develop. In order to calculate what the space charge limited current is as a function of applied field, Poisson's equation must be solved for the particular geometry in question. Assuming an infinite plane parallel electrode geometry, with spacing d , we have a one dimensional problem:

$$\frac{d^2V}{dx^2} = 4\pi n_e e \quad (14)$$

Note that $ne = \frac{j}{ev_d}$, where j is the current density and v_d is the drift velocity of the electrons. The drift velocity can be written in terms of the mean free path as:

$$v_d \approx \left[\frac{2Ve\lambda}{dm_e} \right]^{\frac{1}{2}} \quad (15)$$

Solution of the Poisson equation under these conditions yields an equation of the following form:

$$j = 7.5 \times 10^{-6} \left[\frac{\lambda}{d} \right]^{\frac{1}{2}} \frac{V}{d^2} \quad (\text{amp-m}^{-2}) \quad (16)$$

The derivation of this equation does not take into account additional volumetric ionization in the applied field.

For a given voltage, mean free path, and electrode spacing, j represents the maximum space charge limited current density that can be extracted. In terms of electron density n_e , this expression can be written as:

$$n_e \approx 8 \times 10^7 \left[\frac{V}{d^2} \right] \quad (\text{m}^{-3}) \quad (17)$$

Under our conditions ($V \approx 10$ kV, $d \approx .02$ m), the maximum space charge limited density that can be extracted from the cathode is $\sim 2 \times 10^9$ cm^{-3} . Thus, at a cathode temperature of 1500°C , the full saturated thermionic density of 10^8 cm^{-3} calculated from Richardson's equation can be extracted, and space charge effects are not a limiting factor.

It should be understood that while the results of our experiments are consistent with a thermionic emission process, other effects of cathode heating may contribute to or indeed be responsible for the observed phenomena. For example, transient cathode heating may lead to reduced gas density near the cathode where in effect a low pressure glow discharge may be initiated which then propagates into the higher pressure region in a uniform manner. Such effects have recently been studied in CO_2 laser systems (16). Further work is required to better understand the underlying mechanisms responsible for our observations.

F. Conclusions and Recommendations for Future Work

We have investigated the effects of a heated cathode upon electrical discharge uniformity in several high pressure gases and electro-negative gas mixtures. Spatially uniform TEA discharges have been generated at pd values ≥ 1000 torr-cm using this technique. In addition, preliminary evidence indicates that the electrons emitted from the heated cathode may be used to control the plasma impedance of the discharge.

Although the energy required to pulse heat the cathode to the required temperature may be appreciable, the extent to which this consideration affects the overall efficiency of a laser system depends on the particular system and its properties. For large high energy systems,

the energy put into cathode heating may be a small part of the total energy from an overall system viewpoint.

The most obvious advantage of the thermionic cathode technique for generating uniform discharges lies in its simplicity and low cost compared to existing e-beam and UV preionization techniques.

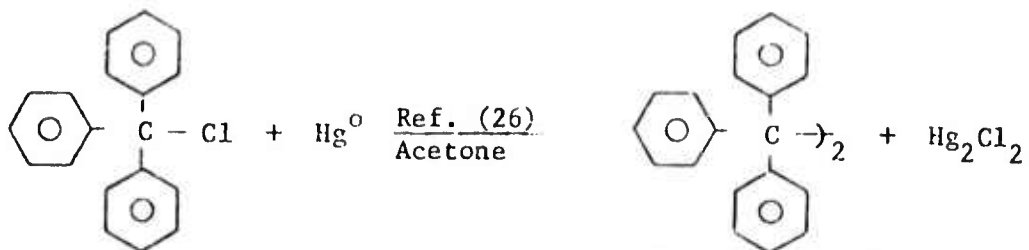
Further work is recommended to incorporate this technique into a rare gas-halogen excimer laser system with the objective of demonstrating high pressure, long pulse operation. In addition, further studies to obtain a more quantitative understanding of the mechanisms responsible for the heated cathode effect are required.

IV. REFERENCES

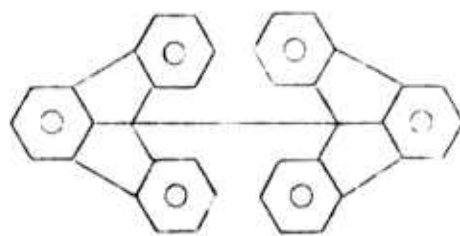
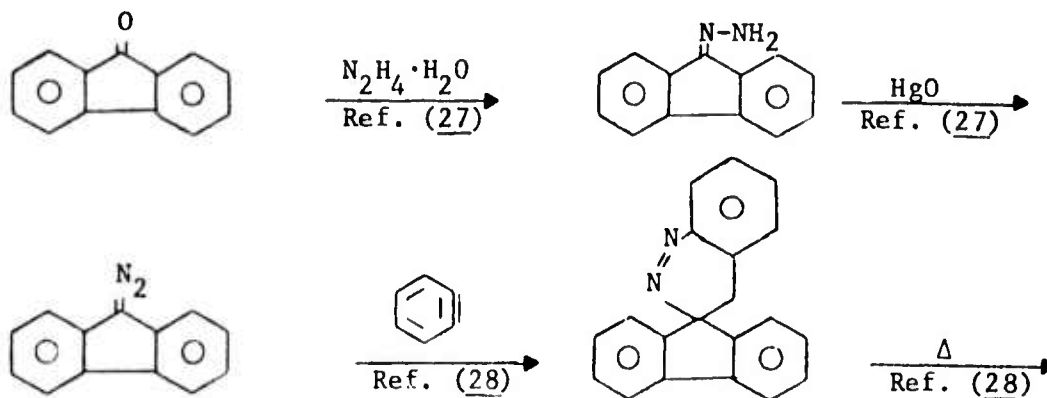
1. A summary of the background information, relevant literature, and pertinent lead references for hexaphenylethane are included in the following sources:
 - a. A. R. Forrester, J.M. Hay and R.H. Thompson, "Organic Chemistry of Stable Free Radicals," Academic Press, Inc., New York (1968).
 - b. C.J.M. Stirling, "Radicals in Organic Chemistry," Oldbourne Press, London (1965).
 - c. G.H. Brown, Ed., "Photochromism," Techniques of Chemistry, Vol. III, Wiley-Interscience, New York (1971).
 - d. Henry Gilman, Ed., "Organic Chemistry--An Advanced Treatise," Vol. 1, 2nd Ed., John Wiley and Sons, Inc., New York, (1963), pp. 581-630.
2. Cankamp, Nauta, and MacLean, Tetra Letts., 2, 249 (1968).
3. Ziegler, Orth, and Weber, Ann. 504, 131 (1935).
4. Ziegler and Ewald, Ann. 473, 169 (1929).
5. G.N. Lewis, D. Lipkin, and T.T. Magel, Trans. Am. Chem. Soc., 66, 1579 (1944).
6. T. Okamura, K. Obi, and I. Tanaka, Chem. Phys. Letts. 20, 90 (1973).
7. W.E. Bachmann and F.Y. Wiselogle, J. Org. Chem. 1, 354 (1936).
8. B.W. Woodward, V.J. Ehlers, and W.C. Lineberger, Rev. Sci. Instr. 44, 882 (1973).
9. G.N. Lewis, and D. Lipkin, J. Am. Chem. Soc., 64, 2801 (1942).
10. J.S. Townsend, Phil. Mag. 3, 557 (1902); 5, 389 (1903); and 6, 598, (1903).
11. L.B. Loeb, "Electrical Breakdown in Gases" in Handbuch der Physik XXII, p. 481, (1956).
12. H. Rafter and E. Flegler, Z. Physik 103, 315 (1936).
13. L.B. Loeb, ibid., p. 473.
14. R.A. Wisjman, Phys. Rev., 75, 833 (1949).
15. A. J. Palmer, Appl. Phys. Lett., 25, 138 (1974).

16. V. N. Karnyushin, A.N. Malov, and R.I. Soloukhin, *Sov. J. Quant. Electron.*, 5, 994 (1976).
17.
 - a. H. P. Leftin and N. N. Lichtin, *J. Am. Chem. Soc.*, 79, 2475 (1957).
 - b. N. N. Lichtin and G. R. Thomas, *J. Am. Chem. Soc.*, 76, 3020 (1954).
 - c. M. Gomberg, *J. Am. Chem. Soc.*, 22, 757 (1900).
 - d. M. Gomberg, *Ber.*, 33, 3150 (1900).
18. G. Baum, R. Bernard and H. Shechter, *J. Am. Chem. Soc.*, 89, 5307 (1967).
19.
 - a. Prepared by cycloaddition of benzyne (2b) with 9-diazofluorene; for general description of synthesis, see ref. (8).
 - b. L. Friedman and F. M. Logullo, *J. Am. Chem. Soc.*, 85, 1549 (1963).
20. M. J. Sabacky, C. S. Johnson, Jr., R. J. Smith, H. S. Gutowsky and J. C. Martin, *J. Am. Chem. Soc.*, 89, 2054 (1967).
21. J. C. Martin and K. G. Smith, *J. Am. Chem. Soc.*, 86, 2252 (1964).
22. W. E. Bachmann, *J. Am. Chem. Soc.*, 55, 2135 (1933).

Hexaphenylethane (A)

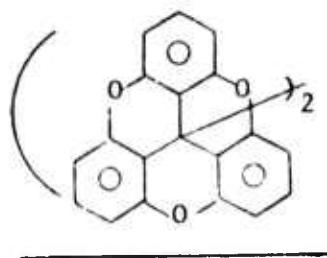
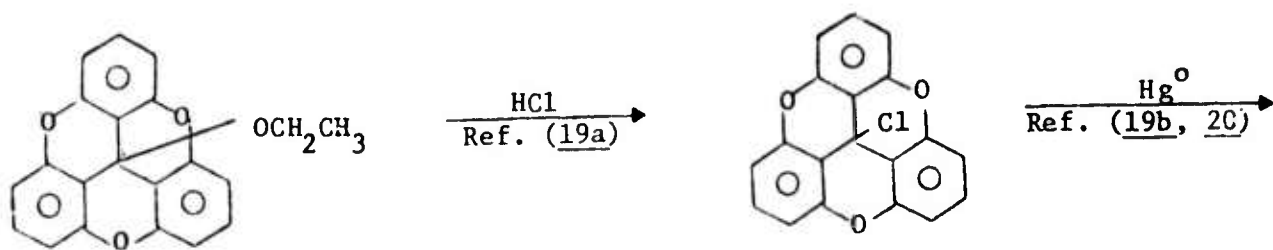
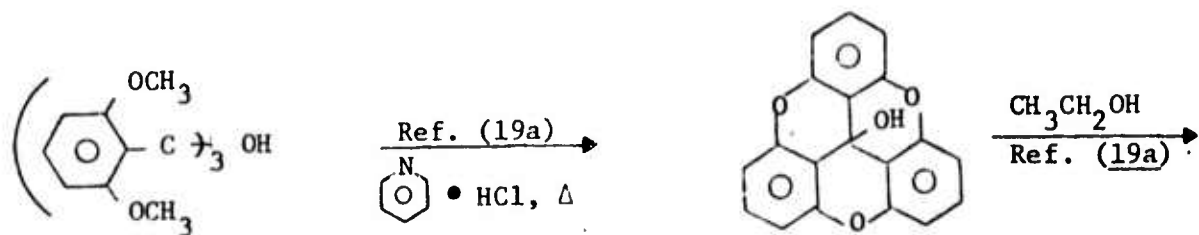
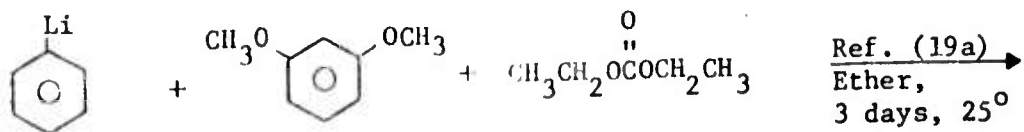


12,12'-Bifluoradene (B)

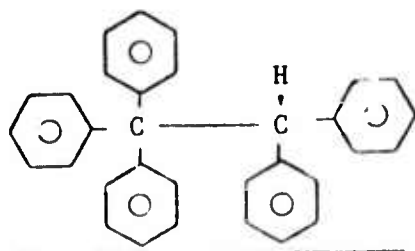
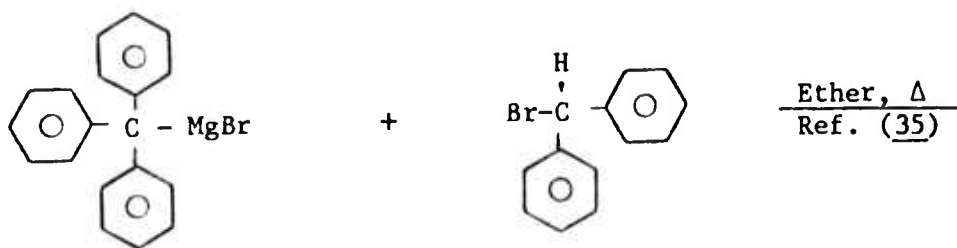


(2-40%, variable yields)

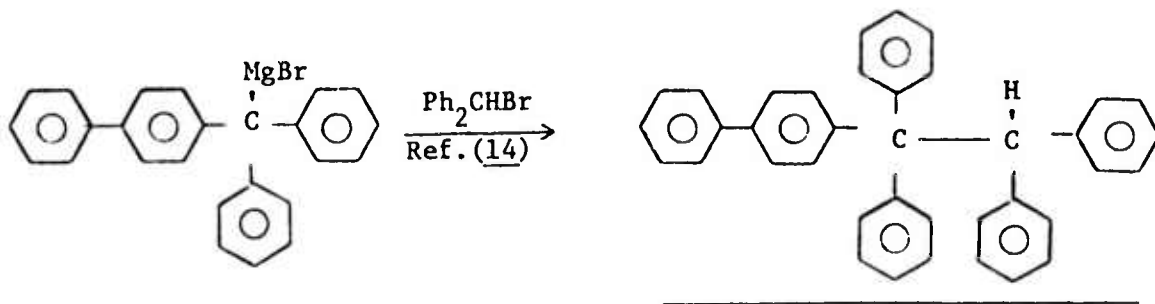
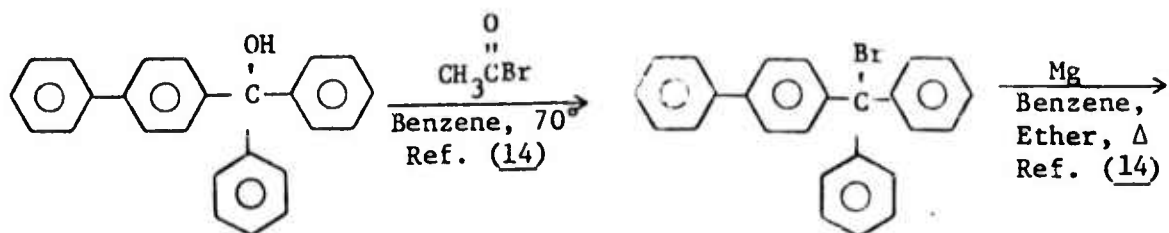
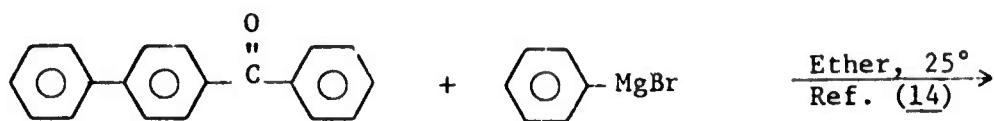
Sesquixanthryl Dimer (C)



Pentaphenylethane (D)



1-p-Biphenyl-1,1,2,2-tetraphenylethane (E)



• Hexaphenylethane (In Situ Preparation)

The starting materials for the in situ preparation of hexaphenylethane were purified in the following manner. Triphenylmethyl chloride was purchased from the Aldrich Chemical Company and was obtained as a colorless crystalline solid after sublimation at 110-115° (0.01 mm). It was stored in a nitrogen-dry box and exposure to the air was kept to the absolute minimum. Spectro-quality 2,2,4-trimethylpentane was purchased from Ace Scientific Supply Company, Inc., and was used as received. Triply distilled, electronic grade mercury was purchased from Alfa-Ventron and was also used as received. All glassware used for the in situ preparation of hexaphenylethane was washed well with acetone, distilled water, dilute hydrochloric acid, dilute ammonium hydroxide, and then finally repetitively washed with distilled water. The excess water was drained from all the glassware, and the reaction flasks, filtering apparatus, etc. were connected to a vacuum rack and evacuated to ca., 10^{-3} mm. by means of an oil diffusion pump. The residual traces of water were then removed by evacuating the glassware for several hours with the intermittent application of external heat via a heat gun.

An "O" ring-sealed, vacuum flask was then charged with the purified triphenylmethyl chloride (0.400 g, 1.435×10^{-3} mole) and about 210 ml of the spectroscopically pure 2,2,4-trimethylpentane. This reaction flask was then sealed by firmly clamping to an "O" ring head which was equipped with two exit vacuum stopcocks. The reaction flask was then attached to the vacuum rack and about 5 ml. of the solvent was removed under reduced pressure. In this manner, most of the dissolved oxygen was removed without recourse to the conventional freeze-pump-thaw cycles. The reaction flask was then transferred to a nitrogen-dry box, and the mercury (10.0 g, 49.8 mmole, 34.7 mole eq.) was added all at once. After sealing the flask, it was completely wrapped with aluminum foil. All ensuing operations were conducted in the complete absence of light or exposure to air. The flask was then reattached to the vacuum system, and the solvent removed under high vacuum to a predetermined 200 ml. mark on the reaction flask. The flask was then sealed under the partial vacuum and was clamped in a horizontal position in a Burrel Model BB, "wrist action" shaker. After shaking for a total of fifteen hours at a constant speed setting of 10, the flask was allowed to stand overnight to allow the inorganic by-product and excess mercury to settle. The clear yellow-orange supernatant was then filtered through a "fine" glass frit into a previously cleaned and evacuated reaction flask. This solution of hexaphenylethane in 2,2,4-trimethylpentane exhibited an absorbance of 0.47 at 5150 Å. It has been stored for a period of 1-2 months in a nitrogen-dry box with no visual loss of color or precipitation of the peroxide. Also, its ultraviolet spectrum was identical to that observed for crystalline hexaphenylethane (17) which was redissolved in degassed solvent.

• 12,12'-Bifluoradene

As reported in the literature (18) a concentrated solution of spiro-(fluorene-9,3'-indazole) (10.0 g, 37.3 mmole) (19) in 80 ml. of decalin was slowly heated to reflux (186°) employing a magnetic stirrer and nitrogen bubbler-cap. The dark solution effervesced fairly vigorously near 170°. This initial reaction subsided after thirty minutes at reflux, and the dark solution was kept at a reflux for a total of one hour. The dark solution was then cooled to room temperature and stirred overnight. The resultant light tan suspension which formed was filtered to afford 12,12'-bifluoradene as a yellow-tan solid in 25% yield (2.2 g, m. pt., 304-306°). This material was obtained in analytically pure form after drying at 50° (0.10 mm) for one day:

Analysis:

Calc. for $C_{38}H_{22}$: C, 95.37; H, 4.63

Found: C, 95.23; H, 4.92

• Sesquixanthryl Dimer

By analogy to the reported procedure (20), reformed sesquixanthryl chloride dihydrate (2.0 g, 5.6 mmole) (21) was dissolved in a mixture of 150 ml. of glacial acetic acid and 10 ml. of concentrated sulfuric acid. A dilute solution of the commercially available chromous chloride (Fisher Scientific Company) was then added dropwise with efficient stirring under a nitrogen atmosphere. A yellow suspension formed immediately upon the beginning of the addition of the chromous chloride solution. The addition was stopped after the reaction mixture assumed a permanent blue color (ca., 120 ml. of $CrCl_2$ solution), and 200 ml. of water was added dropwise. Filtration afforded the crude dimer as a yellowish tan solid in an overall yield of 1.3 g. The analytical pure dimer was obtained after drying at 100° (0.10 mm) for 24 hours (m. pt. 300°).

Analysis:

Calc. for $C_{38}H_{18}O_6$: C, 79.99; H, 3.18

Found: C, 79.18; H, 3.62

• Pentaphenylethane

As previously described in the literature (22) a solution of triphenylbromomethane (32.3 g, 0.10 mole) in 100 ml. of benzene was added dropwise into a suspension of magnesium turnings (2.5 g) in 50 ml. of ether under a nitrogen atmosphere at room temperature. The mixture was then refluxed overnight to complete the formation of the Grignard reagent. The mixture was then cooled to room temperature and the solution was decanted from the unreacted magnesium into a fresh four-neck flask. Solid diphenylbromomethane (27.8 g, 0.10 mole) was then added portion-wise with efficient stirring and cooling with an external water bath. The mixture was then heated for two hours on a steam bath and allowed to stir overnight at room temperature. A 3% solution of acetic acid in water (50 ml.) was then added dropwise with efficient stirring. The organic layer was then separated and the solvent removed under a nitrogen purge. The white solid thus obtained was recrystallized twice from chloroform-ethanol. The analytically pure pentaphenylethane was obtained as a white solid in an overall yield of 12.0 g after drying at 25° (0.10 mm).

Analysis:

Calc. for $C_{32}H_{26}$: C, 93.62; H, 6.38

Found: C, 93.08; H, 6.51

• 1-p-Biphenyl-1,1,2,2-Tetraphenylethane

As reported by Bachmann and Wiselogle (7) diphenyl-p-biphenyl-magnesium bromide was first prepared by heating to reflux a mixture of diphenyl-p-biphenylbromomethane (20.0 g, 1) and magnesium turnings (1.23 g) in 25 ml. of ether and 50 ml. of benzene. The mixture was protected from light by an aluminum foil wrap and was refluxed for a total of ten hours. The characteristic red color of the free radical, diphenyl-p-biphenylmethyl, developed immediately and gradually gave way to the lighter brown color of the Grignard reagent. A solution of the commercially available bromodiphenylmethane (12.35 g) in the minimum quantity of dry benzene was then added fairly rapidly into the reformed Grignard reagent. A moderate exotherm was noted during this addition. The mixture was refluxed for two hours, cooled to room temperature, and then hydrolyzed by the dropwise addition of 100 ml. of 1 M acetic acid. The organic layer was separated and the solvent removed under a nitrogen purge. The dark red oil was then recrystallized three-times for chloroform ethanol. After drying at 80° (0.10 mm) for four hours, the title product was obtained in pure form as a white solid in an overall yield of ca., 3.0 g (m. pt., 173-175°).

Analysis:

Calc. for C₃₈ H₃₀: C, 93.79; H, 6.21

Found: C, 93.36; H, 6.83